Clinical and functional consequences of *GRIA* variants in patients with neurological diseases

Wenshu XiangWei[1,2], Riley E. Perszyk[2], Nana Liu[1,2], Yuchen Xu[2,23], Subhrajit Bhattacharya[2,24], Gil H. Shaulsky[2,3], Constance Smith-Hicks[4,5], Ali Fatemi[4,5], Andrew E. Fry[6,7], Kate Chandler[8], Tao Wang[9], Julie Vogt[10], Julie S. Cohen[4,5], Alex R. Paciorkowski[11,], Annapurna Poduri[12,13], Yuehua Zhang[1], Shuang Wang[1], Yuping Wang[14], Qiongxiang Zhai[15], Fang Fang[16], Jie Leng[17,25], Kathryne Garber[18], Scott J. Myers[2,3], Robin-Tobias Jauss[19,20], Kristen L. Park[21], Timothy A. Benke[21], Johannes R. Lemke[19,20], Hongjie Yuan[2,3*], Yuwu Jiang[1*], Stephen F. Traynelis[2,3,22*]

[1] Department of Pediatrics and Pediatric Epilepsy Center, Peking University First Hospital, Beijing, China

[2]Department of Pharmacology and Chemical Biology, Emory University School of Medicine, Atlanta GA 30322, USA

[3]Center for Functional Evaluation of Rare Variants, Emory University School of Medicine, Atlanta GA 30322, USA

[4]Department of Neurology and Developmental Medicine, Kennedy Krieger Institute, Baltimore MD 21205, USA

[5]Department of Neurology, Johns Hopkins University School of Medicine, Baltimore MD 21287, USA

[6]Institute of Medical Genetics, University Hospital of Wales, Cardiff CF14 4XW, UK

[7]Division of Cancer and Genetics, Cardiff University, Cardiff CF14 4XN, UK

[8]Manchester Centre for Genomic Medicine (MCGM), Manchester University NHS Foundation Trust, Saint Mary's Hospital, Oxford Road, Manchester. M13 9WL, UK

[9]McKusick-Nathans Institute of Genetic Medicine, and Department of Pediatrics, Johns Hopkins University School of Medicine, Baltimore, MD 21205, USA

[10]Department of Clinical Genetics, Birmingham Women's and Children's Hospital (NHS Foundation Trust), Birmingham B4 6NH UK

[11]University of Rochester Medical Center, Child Neurology, 601 Elmwood Ave. Rochester, NY 14642

[12]Epilepsy Genetics Program, Department of Neurology, Boston Children's Hospital, Boston, MA 02115, USA

[13]Department of Neurology, Harvard Medical School, Boston, MA 02115, USA

[14]Department of Neurology, Institute of sleep and consciousness disorders, Center of Epilepsy, Beijing

Institute for Brain Disorders, Beijing Key Laboratory of Neuromodulation, Xuanwu Hospital, Capital Medical University, Beijing, 100053, China

[15]Department of Pediatrics, Guangdong Provincial People's Hospital, Guangdong Academy of Medical Sciences, Guangzhou, China

[16]Department of Neurology, Beijing Children's Hospital, Capital Medical University, National Center for Children's Health, Beijing 100069, China

[17]Department Neurology, Children's Hospital Affiliated to Zhengzhou University/Henan Children's Hospital/Zhengzhou Children's Hospital, Zhengzhou, Henan 450066, China

[18]Department of Human Genetics, Emory University School of Medicine, Atlanta GA 30322 and EGL Genetics, Tucker, GA 30084, USA

[19]Institute of Human Genetics, University of Leipzig Medical Center, Leipzig, Germany

[20]Center for Rare Diseases, University of Leipzig Medical Center, Leipzig, Germany

[21]Departments of Pediatrics and Neurology, University of Colorado School of Medicine and Children's Hospital Colorado, Aurora CO, USA

[22]Emory Neurodegenerative Disease Center, Emory University School of Medicine, Atlanta GA 30322, USA

*Corresponding Authors E-mail addresses: hyuan@emory.edu (HY), jiangyuwu@bjmu.edu.cn (YJ), and strayne@emory.edu (SFT)

[23]Present address: Department of Neurology, the First Hospital of Wenzhou Medical University, Wenzhou, Zhejiang, 325000, China

[24]Present address: School of Pharmaceutical and Health Sciences, Keck Graduate Institute, Claremont Colleges, Claremont, CA 91711 USA

[25]Present address: Department of Endocrinology, Genetics and Metabolism, Chengdu Women's and Children's Central Hospital, School of Medicine, University of Electronic Science and Technology of China. Sichuan 611731, China

Word Count: 5,431

Display Items: 8 (6 figures and 2 tables)

Running Title: Disease associated genetic variants in *GRIA* genes

Abstract

AMPA receptors are members of the glutamate receptor family and mediate a fast component of excitatory synaptic transmission at virtually all central synapses. Thus, their functional characteristics are a critical determinant of brain function. We evaluate intolerance of each *GRIA* gene to genetic variation using 3DMTR and report here the functional consequences of 52 missense variants in *GRIA1-4* identified in patients with various neurological disorders. These variants produce changes in agonist EC_{50}, response time course, desensitization, and /or receptor surface expression. We predict that these functional and localization changes will have important consequences for circuit function, and therefore likely contribute to the patients' clinical phenotype. We evaluated the sensitivity of variant receptors to AMPAR-selective modulators including FDA-approved drugs to explore potential targeted therapeutic options.

Key words: glutamate receptors, channelopathy, *GRIA*, GluA, AMPA, translational study

Introduction

Glutamate receptors mediate excitatory synaptic transmission and can be divided into multiple classes based on pharmacology, structure, and genetic sequence [1]. AMPA receptors (AMPARs) mediate a fast component of the synaptic current and are encoded by *GRIA1-4*. These receptors are in complex with many potential accessory subunits and are embedded into a postsynaptic network of scaffolding and signaling proteins [1]. The actions of AMPARs are essential for normal circuit function, as they are present at virtually all excitatory synapses and are a substrate for activity-dependent post-translational modifications, which are important for synaptic plasticity [1].

The *GRIA* gene family is relatively intolerant to change in comparison to other proteins encoded by the genome, with percentile intolerance scores 5.8, 13, 45, 7.8% for *GRIA1-4*, respectively [2]. Thus, it is not surprising that patients with neurological disease have been found to have missense variants in *GRIA1* [3-7], *GRIA2* [8-11], *GRIA3* [12-21], and *GRIA4* [22]. At present there are over 100 missense *GRIA* variants known [1], although very little information exists regarding the effects of these variants on AMPAR function. Here we evaluate the functional consequences of over 50 AMPAR variants in heterologous expression systems. We additionally report several previously unknown AMPAR variants, along with the associated clinical phenotype. We found a range of different effects on AMPAR properties, all of which we predict will impact circuit function.

Materials and Methods

Consent, study approval, patient phenotype and genetic analysis

This study was approved by the Medical Ethics Committee and the Institutional Review Boards of University of Colorado School of Medicine and Children's Hospital Colorado (COMIRB

16-1520), Peking University First Hospital, John Hopkins University, Birmingham Women's and Children's Hospital, Emory University, and University of Leipzig Hospitals and Clinics. All *in vitro* studies were conducted according to the guidelines of Emory University.

The patient data regarding neurological conditions (i.e., developmental milestones, seizure onset, seizure types, EEG and MRI findings, and response to clinical treatment attempts with conventional antiepileptic drugs) were analyzed retrospectively. Patient-4 (Ala653Ser) and Patient-5 (Val658Ala) (Supplemental Table S1), registered and evaluated by Peking University First Hospital, were identified from a gene panel targeting 480 epilepsy-related genes that included *GRIA1-4*. All other variants were identified by John Hopkins University, Peking University First Hospital, EGL Genetics, Birmingham Women's and Children's Hospital, Manchester University, University of Rochester Medical Center, Boston Children's Hospital, Children's Hospital Colorado, and University of Leipzig Hospitals and Clinics using whole-exome sequencing via commercial clinical laboratories. All genomic DNA used in the experiments were extracted from peripheral leukocytes. All the variants were validated by Sanger sequencing. Assessment of pathogenicity of these variants was performed following ACMG guidelines [23] before functional studies were undertaken. We also collected variants in *GRIA1-4* from patients with epilepsy and developmental/intellectual disability from Pubmed and ClinVar (Table 1).

3DMTR analysis

The 3DMTR (three-dimensional missense tolerance ratio) analysis was performed using a MATLAB (Mathworks, version R2019b) encapsulated application or other custom scripts, all of which are available on GitHub (https://github.com/riley-perszyk-PhD/3DMTR, current version v2.0); annotated pdb files that implement the results of 3DMTR are available in the supplemental information. Only the GluA2 subunits from the open conformation AMPAR structure (PDB:5WEO,

[24]) were used for all *GRIA* genes in the analysis. Variant datasets ("Non-Neuro") for all genes were obtained from the gnomAD website (version 2.1.1). The translated coding gene sequences of GluA1/3/4 were aligned to GluA2 using methods in the Matlab Bioinformatic toolbox to infer which residues correspond to the ones present in the GluA2 structure. This was performed in the application by selecting the gene sequence for GluA2 for the "PDB gene file" and selecting the alternative GluA gene sequence file for the "gnomAD gene file". When both missense and synonymous variant counts were equal to 0, a 3DMTR score of 0 was applied. The alternative structure (O-shaped GluA2/GluA3 receptor, PDB:5IDE, [25]) was used to examine the 3DMTR of GluA3.

Molecular biology

Mutagenesis was performed on complementary DNA (cDNA) encoding human *GRIA* genes [26] using the QuikChange protocol with Pfu DNA polymerase (Stratagene La Jolla, CA, USA) to replicate the parental DNA strand with the desired mismatch incorporated into the primer. Methylated parental DNA was digested with Dpn I for 3 hours at 37˚C and the nicked mutant DNA was transformed into TOP10 Competent Cells (Life Tech, Grand Islands, NY, USA). Bacteria were spun down and prepared using the QIAGEN QIAprep Spin Miniprep Kit (Hilden, Germany). Sequences were verified through the mutated region using dideoxy DNA sequencing (Eurofins MWG Operon, Huntsville, AL, USA). The plasmid vector for wild type (WT) human GluA1-4 (GenBank accession codes: NP_001107655, NP_000817, NP_015564 and NP_015566) was pCI-neo and for human Stargazin/CACNG2 (GenBank accession codes: NP_006069, generously provided by Janssen Research and Development) was pcDNA3.1.

We utilized the following Leu-Tyr mutations at the agonist binding domain dimer interface to reduce desensitization [27] for some experiments: *GRIA1* (NM_001114183, Leu497Tyr, *GRIA3*

(NM_007325, Leu513Tyr), *GRIA4* (NM_000829, Leu505Tyr). We also modified the Arg encoded at the editing site in the M2 reentrant pore loop mRNA to Gln to match the genomic sequence for *GRIA2* (NM_000826, Arg607Gln; [28,29,1]). All clones contained the flip splice variant [30].

The cDNA was linearized using FastDigest (Thermo, Waltham, MA) restriction digestion at 37°C for 1 hour. Complementary RNA (cRNA) was synthesized *in vitro* from linearized cDNA for WT and mutant AMPAR subunits using the mMessage mMachine T7 kit according to manuufacturer's instructions (Ambion, Austin, TX, USA). *Xenopus laevis* stage VI oocytes were prepared from commercially available ovaries (Xenopus one Inc, Dexter, MI, USA). The ovary was digested with Collagenase Type 4 (Worthington-Biochem, Lakewood, NJ, USA) solution (850 μg/mL, 15 ml for a half ovary) in Ca^{2+}-free Barth's solution, which contained (in mM) 88 NaCl, 2.4 $NaHCO_3$, 1 KCl, 0.82 $MgSO_4$, 10 HEPES (pH 7.4 with NaOH) supplemented with 100 μg/ml gentamycin, 1 U/ml penicillin, and 1 μg/ml streptomycin. The ovary was incubated in enzyme with gentle mixing at room temperature (23°C) for 2 hours. The oocytes were rinsed 5 times with Ca^{2+}-free Barth's solution (35-40 mL of fresh solution each time) for 10 min each time, and further rinsed 4 times with 35-40 mL of fresh normal Barth's solution, which included 0.33 mM $Ca(NO_3)_2$ and 0.41 mM $CaCl_2$, on the mixer for 10 min each time. The sorted oocytes were kept in 16°C incubator for further use. *Xenopus laevis* oocytes were injected with AMPAR cRNA that by weight was 5-10 ng in 50 nL of RNase-free water per oocyte [26]. Injected oocytes were maintained in normal Barth's solution at 15-19°C.

Two-electrode voltage clamp current recordings

Two-electrode voltage clamp (TEVC) current recordings were performed two to three days' post-injection at 23˚C, as previously described [26,31]. The extracellular recording solution contained (in mM) 90 NaCl, 1 KCl, 10 HEPES, 1.0 $BaCl_2$, and 0.01 EDTA (pH7.4 with NaOH).

Solution exchange was computer-controlled through an 8-valve positioner (Digital MVP Valve, Hamilton, CT, USA). Oocytes were placed in a dual track chamber that shared a single perfusion line, allowing simultaneous recording from two oocytes. All concentration-response solutions were made by adding agonists to the extracellular recording solution. Voltage control and data acquisition were achieved by a two-electrode voltage-clamp amplifier (OC725C, Warner Instruments, Hamden, CT, USA). The voltage electrode was filled with 0.3 M KCl and the current electrode with 3 M KCl. Oocytes were held under voltage clamp at holding potential -40 mV unless otherwise indicated. All chemicals were obtained from Sigma-Aldrich unless otherwise stated.

Whole-cell voltage-clamp current recordings

Human embryonic kidney (HEK 293) cells (ATCC CRL-1573; Manassas, VA, USA) were plated on glass coverslips pre-treated with 0.1 mg/ml poly-D-lysine and cultured in DMEM/GlutaMax medium (GIBCO, 15140-122) supplemented with 10% fetal bovine serum and 10 U/ml penicillin and 10 μg/ml streptomycin at 37°C and maintained in a humidified environment with 5% CO_2. The HEK cells were transiently transfected with plasmid cDNAs encoding WT or mutant human AMPAR along with GFP at a cDNA ratio of 1:1 (0.2 – 0.4 μg/μL) by using the calcium phosphate precipitation method [32,33,26]. After 48 hours following the transfection, the cells on coverslips were moved to a submerged recording chamber with continuous perfusion with external recording solution that contained (in mM) 3 KCl, 150 NaCl, 0.01 EDTA, 1.0 $CaCl_2$, 10 HEPES, and 11 D-mannitol, with the pH adjusted to 7.4 by NaOH. External solution was filtered through 0.45 μm nylon filters under vacuum. The whole-cell voltage-clamp current recordings were performed with fire polished recording electrodes with a resistance of 3-4 MΩ that were made of thin-walled filamented borosilicate glass (TW150F-4, World Precision Instruments, Sarasota, FL, USA) filled with the internal pipette solution that contained (in mM) 110 D-gluconic acid, 110

CsOH, 30 CsCl, 5 HEPES, 4 NaCl, 0.5 $CaCl_2$, 2 $MgCl_2$, 5 BAPTA, 2 Na_2ATP, 0.3 Na_2GTP; pH was adjusted to 7.4 with CsOH and the osmolality was adjusted to 300-310 mOsmol/kg using CsCl or water. The whole cell current responses were evoked by the rapid application of maximally effective concentrations of agonists (10 mM glutamate for 5 ms, 100 ms, or 1 s) at a holding potential of -60 mV and recorded using a Axopatch 200B patch-clamp amplifier (Molecular Devices, CA, USA). For each cell, solution exchange time was measured using changes in the junction potential at the electrode tip when normal extracellular solution and diluted solution were flowing through each side of a theta tube, and adjusted to be less than 1 ms before experiments. The current responses were anti-alias filtered with -3 dB, 8 pole Bessel filter at 8 kHz (Frequency Devices, IL, USA) and digitized at 20 kHz using Digidata 1440A acquisition system (Molecular Devices, CA, USA) controlled by Clampex 10.3 (Molecular Devices, CA, USA).

Beta-lactamase assay

HEK293 cells were plated in 96-well plates (50,000 cells per well) and transiently transfected with cDNA encoding WT or mutant β-lac-GluA1, β-lac-GluA2 and β-lac-GluA4 (homomeric receptors), or β-lac-GluA3 with WT GluA2 and human stargazin (γ-2) at a cDNA ratio of 1:1:1 using Fugene6 (Promega, Madison, WI), as previously described [34]. Cells treated with Fugene6 alone were used to define background signal. Briefly, six wells were transfected for each condition; surface and total protein levels were measured in three wells each. After 24 hours, cells were rinsed with Hank's Balanced Salt Solution (HBSS, in mM, 140 NaCl, 5 KCl, 0.3 Na_2HPO_4, 0.4 KH_2PO_4, 6 glucose, 4 $NaHCO_3$) supplemented with 10 mM HEPES, and then 100 μL of a 100 μM nitrocefin (Millipore, Burlington, MA, USA) solution in HBSS with HEPES added to each well for measuring the level of extracellular enzymatic activity, which reflected AMPAR surface expression. To determine the level of total enzymatic activity, the cells were lysed by a 30-min

incubation in 50 μL H_2O prior to the addition of 50 μL of 200 μM nitrocefin. The absorbance at 486 nm was assessed using a microplate reader every min for 30 min at 30℃. The rate of increase in absorbance was generated from the slope of a linear fit to the data.

Evaluation of AMPAR positive or negative modulators

The concentration-response relationships for AMPAR positive allosteric modulators (CX-614, Aniracetam, cyclothiazide) or negative allosteric modulators (CP-465,022, perampanel, GYKI52466, GYKI53655) and competitive antagonists (NBQX) were evaluated using TEVC recordings from *Xenopus* oocytes expressing WT or mutant GluA1-4 at a holding potential of -40 mV. The averaged current response amplitudes were fitted with *Equation 1* to determine the EC_{50} values and *Equation 2* to determine the IC_{50} values (*see* below).

Data and statistics analysis

The data supporting the findings of this study are available within the article and its supplementary material. Raw data and derived data supporting the findings of this study are available from the corresponding author upon request.

Statistical analyses were performed in GraphPad Prism 5 (La Jolla, CA, USA) and OriginPro 9.0 (Northampton, MA, USA). Statistical significance was assessed using one-way ANOVA with Post hoc Dunnett's Multiple Comparison Test, with $p < 0.05$ considered significant. Power was determined using Gpower (3.1.9.2). Data are presented as mean ± SEM. Error bars represent SEM unless otherwise stated. The concentration-response relationship for agonists were fitted by

$$Response = 100\% / (1 + (EC_{50} / [\ agonist\ ])^{N}) \quad \text{Eq. 1}$$

and the concentration-response relationship for inhibition was fitted by

$$Response = (100\% - minimum) / (1 + ([\ concentration\ ] / IC_{50})^{N}) + minimum. \quad \text{Eq. 2}$$

N is the Hill slope, EC_{50} is the concentration of the agonist that produces a half-maximal effect, IC_{50} is the concentration of the inhibitor that produces a half-maximal effect, and *minimum* is the degree of residual current observed at a saturating concentration of the inhibitor.

The deactivation time course following rapid removal of glutamate after prolonged application was fitted by a non-linear least squares algorithm (ChanneLab, Synaptosoft, Decatur, USA) with a two-component exponential function,

$$Response = Amplitude_{FAST}\,(exp(-time/\tau_{FAST})) + Amplitude_{SLOW}\,(exp(-time/\tau_{SLOW})). \quad \text{Eq. 3}$$

For desensitization time courses fitted by a single exponential function, *Equation 3* was used with $Amplitude_{SLOW}$ set to be 0. For dual exponential fits, the weighted average tau was calculated as

$$\tau_{weighted} = (Amplitude_{FAST}\ \tau_{FAST} + Amplitude_{SLOW}\ \tau_{SLOW}) / (\ Amplitude_{FAST} + Amplitude_{SLOW}\ ). \quad \text{Eq. 4}$$

For some experiments in which the whole cell current response to brief application of glutamate was measured, we fitted the deactivation time course to two exponential functions with the tau for one component (τ_{SLOW}) fixed to the time constant determined from analysis of the desensitization time course, which was obtained from responses to prolonged glutamate application on the same cell. We then reported τ_{FAST} as the deactivation time constant.

Results

GRIA variants identified in patients with neurological conditions

We report here 14 novel *GRIA* missense variants that were identified in patients with neurological conditions (Table 1). These variants included 2 *GRIA1, 4 GRIA2, 6 GRIA3,* and 2 *GRIA4* missense variants. We also studied an additional 38 variants identified in the literature and ClinVar. The clinical phenotypes of these patients include epilepsy, intellectual disability, microcephaly, sleep disorders, autistic features, language problems, movement disorders, and/or behavioral abnormalities (Table 1, Fig. 1, Supplemental Table S1). The ACMG classification is

provided in Supplemental Table S1. Five of these 52 variants were present in the general population (gnomAD database, checked on March 2023), including *GRIA3*_p.Ile36Val, *GRIA3*_p.Met261Ile, *GRIA3*_p.Ala337Gly, *GRIA3*_p.Arg450Gln, and *GRIA4*_p.Arg697Gln. The *GRIA3* gene is located on Chromosome X, and it is possible that some variants can be carried by healthy females in the population. The *GRIA2* and *GRIA4* variants found in gnomAD alter receptor function (*see* below), however it is unclear what the consequences are for this. Most of the variants in this study are candidates for potential contribution to the clinical phenotype, but functional data for these variants are limited. We therefore introduced each variant into cDNA for the relevant human *GRIA1-4* genes and studied the functional and biochemical properties of the AMPARs in heterologous expression experiments.

Tolerance analysis to genetic variation for genes encoding AMPA receptor subunits

Using the near full length open conformation structure (PDB:5WEO [24]) we can calculate the 3DMTR [35] for portions of the receptor represented in the structure for each gene (Fig. 2, Supplemental Fig. S1, Supplemental 3DMTR structural file). In general, each gene has a 3DMTR pattern that is distinct from the others but with some shared general trends. Each *GRIA* gene typically has intolerant hotspots in portions of the ABD (agonist binding domain), TMD (transmembrane domain), and at the apex of the NTD (amino-terminal domain) (Fig. 3). As these genes encode ion channels, this result is not unexpected, given that these portions of the receptor have important functions such as agonist binding and channel gating, which are evident in the 3DMTR profile. It is noteworthy that M1 and M4 transmembrane helices interact with auxiliary subunits (e.g. TARPs, GSG1L, cornichons, Supplemental Fig. S2, [36,1]). The M1 transmembrane helix of GluA1,2,4 and the M4 transmembrane helix of GluA1 are intolerant to variation, which for some variants might reflect the importance of AMPAR-auxiliary subunit interactions for normal

brain function. Interestingly, there is an intolerant region in the NTD for GluA1-3 that suggests critical residues for NTD dimerization or a potential interaction with a trans-synaptic binding partner (Fig. 3). This intolerant NTD site seems the clearest in GluA1 and GluA2, whereas GluA3 has a different pattern. GluA3 may form protein complexes in a heterotetramer with GluA2, which has been suggested to have an alternative conformation [25]. The alternative structures associated with these different conformations provide a similar overall 3DMTR, but reorient this intolerant site, suggesting that the intolerance involves NTD dimer interactions as well as inter-NTD dimer interactions (Supplemental Fig. S3).

There are some distinctions in each *GRIA*/GluA protein that may illuminate differential functions. GluA1 has intolerant M4 and NTD regions (Fig. 3). GluA2 has intolerant ABD, TMD (especially M1, M2, M3), and NTD regions (Fig. 3). GluA3 has an intolerant ABD, ABD-TMD linkers, and a wider NTD region (Fig. 3). GluA4 has an intolerant ABD (especially the dimer interface) and M3 (Fig. 3).

The *de novo* variants discussed in this work generally are found in regions that lack missense variants in the general population, which corresponds to regions with lower, more intolerant 3DMTR scores (Fig. 2B, Supplemental Fig. S4). GluA1 has an average 3DMTR of 0.65 ± 0.01 (n = 793), whereas the *de novo* variant sites have an average 3DMTR of 0.41 ± 0.09 (n = 4). GluA2 has a average 3DMTR of 0.57 ± 0.01 (n = 793) that is similar to the average 3DMTR for variants of 0.48 ± 0.12 (n = 6). GluA3 has an average 3DMTR of 0.56 ± 0.01 (n = 793), whereas the *de novo* variant sites have an average 3DMTR of 0.42 ± 0.06 (n = 29). GluA4 has an average 3DMTR of 0.75 ± 0.01 (n = 793), whereas the *de novo* variant sites have an average 3DMTR of 0.39 ± 0.10 (n = 6). Thus, in each case the 3DMTR score of the *de novo* missense variants are on average lower than that of the entire protein, although this difference appears modest for GluA2. The locations of these *de novo* variants therefore appear to have the potential to be functionally

consequential when altered.

Effects of *GRIA* missense variants on agonist potency

We first evaluated the potency for agonist activation of variant-containing GluA1-4 receptors. We observed current responses in 46 of 52 variants expressed in *Xenopus* oocytes during the application of glutamate; the remaining 6 variants did not produce measurable current responses. We subsequently recorded concentration-response curves for steady-state responses to glutamate and kainate on these variants. Figure 4 shows representative glutamate concentration-effect curves for several *GRIA1*, *GRIA2*, *GRIA3*, and *GRIA4* variants determined in *Xenopus* oocytes expressing homomeric AMPARs, and illustrates a range of effects of the variants on agonist potency. We find both variant-induced increases and decreases in glutamate potency for GluA1, GluA3, and GluA4. By contrast, we found only two variants that significantly increased glutamate potency at GluA2. Table 2 summarizes the EC_{50} values determined for these variants. We observed a significant increase in glutamate potency (decreased EC_{50}) for GluA1-A636T, for GluA2-E508V, -V647A, -V647L, for GluA3-S527R, -V560A, -S647F, -A653S, -V658A, -R660S, -G803E, -A818T, and for GluA4-T639S, -N641D, -A643G, -A644V. By contrast, we observed a decrease in glutamate potency (increased EC_{50}) for GluA1-T663M, for GluA3-M617T, -A653T, -F655S, -M706T, -L774S, -G806S, -T816I, and for GluA4-R697P, -R697Q. We also measured the concentration-response relationship for the partial agonist kainate at all variant receptors (Supplemental Fig. S5). Whereas we were unable to record measurable responses to kainate at human GluA1, the effects of variants in other *GRIA* genes on the EC_{50} value for kainate activation were similar, but not identical to that observed for glutamate. Table 2 compares the EC_{50} values for both kainate and glutamate at all variant receptors. Several variants showed differential effect on glutamate and kainate potency (e.g. GluA3-T816I and GluA3-M706L), which may suggest actions

on the process of desensitization (Table 2).

Variants that altered potency of agonist were identified in the ABD, as expected since this region controls the association and dissociation rates for glutamate (Table 2). In addition, some variants in ABD-transmembrane domain linkers also altered agonist potency, which would be consistent with effects on agonist EC_{50} secondary to changes in efficacy [37]. The linkers are known to influence efficacy given they directly connect the agonist binding site to the channel gate. In addition, a number of variants in the pore-forming regions also influence agonist potency, again most likely secondary to actions on gating (Table 2).

Effects of *GRIA* missense variants on AMPA receptor response time course

We subsequently chose three *GRIA4* variants (GluA4-T639S, GluA4-A643G, and GluA4-A644V) and eleven *GRIA3* variants (GluA3-M617T, GluA3-S647F, GluA3-A653S, GluA3-A653T, GluA3-T655S, GluA3-V658A, GluA3-R660S, GluA3-M706T, GluA3-G803E, GluA3-G806S, GluA3-T816I) to study at higher temporal resolution in HEK293 cells in response to rapid application of maximally effective concentrations of glutamate (10 mM). Figure 5A and Supplemental Table S2 shows three *GRIA4* variants that all reduce either the extent or rate of desensitization in response to prolonged application of glutamate. Homomeric WT GluA4 exhibited a τ_{FAST} of 5.8 ± 0.5 ms and a steady-state/peak current ratio (SS/Peak) of 0.02 ± 0.01 (n = 14). The time course of desensitization for the WT GluA4 could be fit with a single exponential function and showed a typical time constant for AMPAR desensitization. However, the GluA4-T639S variant possessed a $\tau_{weighted}$ for desensitization of 27 ± 1.3 ms and SS/Peak ratio of 0.78 ± 0.044 (n = 3). GluA4-A643G and GluA4-A644V variants showed SS/Peak of 0.92 ± 0.004 (n = 6) and 0.98 ± 0.006 (n = 5), respectively, with $\tau_{weighted}$ for desensitization undetermined. GluA4-A643G and GluA4-A644V variants showed prolonged deactivation time course upon removal of

glutamate ($\tau_{weighted}$ for deactivation was 41 msec and 94 msec, respectively) compared to that of WT receptors (5.1 msec). Given the slower time course of desensitization and/or deactivation, each of these variants is predicted to have a prolonged response to glutamate at central synapses, provided glutamate endures in the synaptic cleft long enough to produce a certain degree of desensitization (e.g., [38]).

The *GRIA3* variants tested showed more modest differences in response time course compared to WT *GRIA3* (Supplemental Fig. S6, Supplemental Table S3). We recorded the response to brief and prolonged application of 10 mM glutamate onto cells expressing WT or variant receptor. We used whole cell recordings from HEK cells co-transfected with GluA3 cDNA and the auxiliary subunit TARP γ2 due to low expression of GluA3 in transfected HEK cells without TARPs. We fitted the desensitization time course with a single exponential function for responses to prolonged glutamate application. For the brief glutamate application experiments, the exchange time around a whole cell is slow, on the order of several milliseconds. Thus, our measured deactivation time constants may systematically overestimate the true deactivation time course since they will contain a slow component corresponding to slow removal of glutamate from around the cell. To circumvent the convolution of the desensitization and deactivation rates, we fitted the decay of these current responses with dual exponential function where one tau was fixed to that found for desensitization in the same cell measured in response to prolonged application of glutamate. We interpreted the other time constant as reflective of the deactivation time course. From these experiments we identified 5 variants that altered the response time course. GluA3-T655S showed an accelerated desensitization time course compared to WT. GluA3-S647F showed an accelerated deactivation rate compared with WT. GluA3-M617T and GluA3-M706T enhanced the extent of desensitization (i.e. smaller SS/Peak ratio) compared to WT. Further investigation of variants in AMPAR in which desensitization has been removed by site directed mutagenesis of key

residues may provide additional information on how variants impact deactivation.

Effects of *GRIA* missense variants on AMPA receptor surface expression

We also tested whether these variants could alter the total expression of AMPAR receptors or the number of receptors that reached the cell surface. We created a fusion protein between β-lactamase (β-lac) and each AMPAR cDNA, with β-lac placed in-frame at the N-terminus [34]. We subsequently introduced each variant into the parent β-lac-construct, and transfected HEK cells with either WT or variant cDNA. We then incubated intact cells with a colorimetric substrate and monitored the conversion of substrate to product (*see* Methods). Figure 5B-E shows the conversion of substrate to product as a function of time for WT and representative variants for each AMPAR subunit (*left panels*) and the degree of β-lac activity in variant and WT receptors (*right panels*). The levels of total AMPAR protein expression and AMPAR surface expression are summarized for all variants in Table 2. Virtually all variants showed some degree of surface expression, even those without measurable responses in oocytes. However, the majority of these variants reduced the levels of receptors that reached the surface of HEK cells as detected with this assay. We interpret these data to suggest that many of these variants may also compromise surface expression in neurons.

Response of *GRIA* variants to allosteric modulators and competitive antagonists

GRIA variants that reduce receptor function could be amenable to enhancement by a class of positive allosteric modulators often referred to as AMPAkines (Supplemental Table S4). We selected a subset of *GRIA2-4* variants (GluA3-F655S, GluA3-M706T, and GluA4-R697P) that either reduced agonist potency or surface expression, or both. We subsequently compared the effect of a single concentration of three modulators (CX-614, aniracetam, cyclothiazide, *see* [1]) that enhance AMPAR charge transfer by either diminishing desensitization, prolonging deactivation, or

both. Figure 6A-C summarizes the actions of these agents and shows that CX-614 and cyclothiazide both retain their ability to enhance the steady-state responses to glutamate in WT and variant AMPARs expressed in *Xenopus* oocytes. The concentration-response relationship for CX-614 is unchanged for the *GRIA4* variant R697P. None of the variants tested responded to a subthreshold concentration of aniracetam, consistent with the idea that variants did not show enhanced sensitivity to this positive allosteric modulator (Fig. 6B).

We subsequently selected a subset of variants that appear to enhance AMPAR responses either by increasing agonist potency or reducing the degree of desensitization (GluA3-G803E, GluA4-T639S, GluA4-N641D, GluA4-A643G). We evaluated the effects of a single concentration of the negative allosteric modulators perampanel, GYKI-52466, GYKI-53655, and CP-465,022 on the steady-state response to glutamate at variant AMPARs (Fig. 6D-G, Supplemental Table S5). We also assessed the effects of the AMPA/kainate receptor competitive antagonist NBQX on these variants (Fig. 6H). The variant GluA3-G803E showed a similar degree of block by all inhibitors, and identical concentration-response relationships for these inhibitors (Fig. 6I,K). The response for GluA4 variants was more complex, with some showing a similar sensitivity to inhibitors, whereas others were less sensitive (Fig. 6D-H). This was reflected in the concentration-dependence of these inhibitors assessed at GluA4 variants (Fig. 6J,L, Supplemental Table S6).

Discussion

Identification of *GRIA* variants as potentially disease-associated is an important new development in pediatric neurology and presents an opportunity to better understand a subset of previously undiagnosed neurodevelopmental disorders. The most important result of this study is the demonstration that many of the AMPAR variants produce measurable changes in functional properties for AMPARs expressed in heterologous systems, suggesting these changes could

contribute to clinical characteristics through alterations in AMPAR properties that influence circuit and brain function. It will be important to evaluate functional effects of AMPAR variants in neurons to determine whether the functional consequences of missense variants determined in expression systems are present in a neuronal context.

At present there is no way to predict *a priori* whether a variant will produce a functional change, or what direction that will be, making work that connects changes in receptor function to clinical characteristics necessary. We observed that most *de novo* variants occur at residues that have more intolerant 3DMTR scores and that variants that alter glutamate EC_{50} are clustered in the ABD and the TMD (Supplemental Fig. S7). Clinically, assessment of location and 3DMTR scores could be useful in absence of functional characterization when assessing pathogenicity of missense variants. With further identification and functional characterization of novel *de novo* variants in *GRIA* genes, spatial patterns of functional alterations from receptor variants may become apparent.

The large effects some variants have on AMPAR properties seem likely to impact clinical phenotype. However, we do not know what degree of change in various receptor properties is tolerated in the healthy population. This gap in our understanding makes it difficult to assess, for example, whether a 2-fold change in glutamate potency is meaningful. Moreover, for some AMPAR variants, modest changes in potency that might increase overall charge transfer could be offset by reductions in surface expression. Furthermore, we see that variants can have complex array of effects on AMPA receptor activation, deactivation, and desensitization that may not be comparable between GluA subunits. A systematic evaluation of a comprehensive set of functional properties is needed to begin to categorize the effects at least on synaptic function. While a comprehensive evaluation of how a missense variant might impact overall net function has been proposed for NMDA receptor variants [39], this has not been done yet for AMPARs. Indeed, systematic evaluation of the overall net consequences of multiple changes in AMPAR functional

properties will be more complex than NMDARs, given that incorporation of GluA2 into the tetrameric complex and association of different classes of accessory subunits to markedly change AMPAR properties.

An additional complication with interpretation of these results is the nature of contribution that variant AMPAR subunits make on tetrameric receptors. For X-linked *GRIA3* variation, one will expect all GluA3 subunits to carry the variant in males, and thus there could be receptors with any number of GluA3 variant subunits, potentially including homomeric GluA3 receptors similar to those studied here. However, for *GRIA1*, *GRIA2*, and *GRIA4* variants, there will be fewer variant subunits in a typical AMPAR complex due to heterozygosity than for the recombinant receptors expressed here. Thus, the functional changes observed in patient AMPARs will almost certainly be more modest than what we observe, unless a variant has a dominant effect on receptor function. However, AMPARs seem capable of allowing individual subunit contributions to gating (e.g. [40,41]), which means WT subunits should be able to exert an influence on receptor properties when only a single variant subunit is present.

We also observed that the M1 transmembrane helix in GluA1, GluA2 and GluA4 showed intolerance to variation, which indicates some variants in this region could potentially alter the interaction of AMPARs with auxiliary subunits such as TARPs, cornichons, and GSG1L in a manner that impairs circuit function [36]. The GluA1 M4 region also showed intolerance, which is also consistent with potential interaction with auxiliary subunits. This possibility can be assessed by evaluating the effects of variants in M1 and M4 on a wide range of AMPAR functional properties that are influenced by accessory subunits [1]. Exploration of variants in the various accessory subunits may yield additional information.

The functional assessment described here is necessary for the categorization of effects as potentially gain- or loss-of-function, a simplistic but useful classification that can be instructive in

determining potential treatment strategies. For example, variants that clearly alter AMPAR activation raise the possibility of testing various AMPAR-selective modulators, and determining the net effect of the variant can help identify the best potential strategy. Multiple examples of compounds that inhibit or enhance AMPAR function exist [1], some of which have been shown to be safe in children [42-44]. We report the actions of a number of pharmacological agents on the function of variant AMPARs. At least one of these agents (perampanel) has been clinically approved for use as antiseizure medication, and it seems possible that some benefit might be derived in patients with strong gain-of-function AMPAR variants, provided AMPARs containing those variant subunits retain sensitivity to perampanel [45]. Other agents such as CX-614 are in classes of compounds often referred to as AMPAkines that have been studied in the clinic, raising the possibility that select AMPAkines might find utility in treating conditions arising from variant AMPARs with diminished function. These drugs may allow an attenuation of AMPAR over-activation or enhancement of AMPAR hypofunction, either of which may partially rectify circuit imbalances that result from AMPAR dysfunction. This is important given the recent connection of *GRIA3* variants to schizophrenia [46]. Our data support the idea that a subset of AMPAR variants will retain sensitivity to these agents, and thus it is a potential path forward for treatment. While these studies raise this idea as a possibility, considerably more work at the pre-clinical stage both *in vitro* and *in vivo* is necessary to evaluate the full potential of these candidate precision therapies.

Clearly more data is needed to understand the implications of these functional changes, and how they contribute to disease phenotype. We expect that further study on *GRIA* variants will be instrumental in allowing clinical diagnostic criteria to be developed, which will facilitate better identification and treatment of patients with these variants.

Supplemental information

Supplemental Table S1: Clinical features and genetic characteristic of patients with *GRIA* variants

Supplemental Table S2: Summary of rapid activation, desensitization, and deactivation of GluA4 variant receptors

Supplemental Table S3: Quantified summary of rapid activation and deactivation of GluA3 variant receptors

Supplemental Table S4: Summary of rescue pharmacology for loss-of-function variants

Supplemental Table S5: Summary of rescue pharmacology for gain-of-function variants (single concentration assay)

Supplemental Table S6: Rescue pharmacology for gain-of-function variants (concentration response assay)

Supplemental Figure S1: 3DMTR scores of the GluA1-4 receptors

Supplemental Figure S2. Stargazin interacts primarily with the M1 and M4 helices

Supplemental Figure S3: Alternative GluA3 3DMTR score based on the O-shaped AMPA structure

Supplemental Figure S4: Location of *de novo*, missense, and synonymous variants on each GluA subunit

Supplemental Figure S5: The variant GluA2-4 receptors change kainate potency

Supplemental Figure S6: Rapid activation and deactivation of GluA3 variant receptors expressed in HEK293 cells

Supplemental Figure S7. Location of tested *GRIA* variants that have altered and unaltered glutamate EC_{50}

3DMTR Pymol file showing color-coded intolerant/tolerant regions for AMPARs: A pymol session file containing all four *GRIA* genes 3DMTR colored for intolerant (blue) and tolerant (red) regions mapped onto the GluA2 model (pbd:5WEO) as described in the text is included for users to make figures. The alternative GluA2/GluA3 structure is also included (pdb:5IDE). The structures, for each GluAX, contained in this file are named as "GluAX_3DMTR_intraReceptor_closest31residues_nonNeuro". Please cite this paper if you make and use images from this file.

Acknowledgements We thank Jing Zhang and Sukhan Kim for their excellent technical support

and Janssen Research and development for providing the human TARP gamma-2 cDNA.

Authors' contributions HY, YJ, and SFT designed the study and analyzed the data. CSK, AF, AF,

KC, TW, JV, JSC, ARP, AP, YZ, SW, YW, QZ, FF, JL, KG, RTJ, KLP, TAB, JL, and YJ conducted the neuropsychological assessment, performed the genetic analyses, and/or reviewed the patients' clinical histories. WX, REP, NL, YX, SB, GHS, and SJM conducted functional studies and analyzed the data. All authors wrote and approved the manuscript.

Funding This work was supported by the NIH (NS111619 to SFT; MH127404 to HY; HD103538 to JSC), the CureGRIN Foundation to SFT, and by the University Research Committee (Emory URC, #00085889 to HY).

Data availability The datasets generated during and/or analyzed during the current study are available from the corresponding author on reasonable request.

Declarations

Conflict of Interest statement SFT is a member of the SAB for Sage Therapeutics, Eumentis Therapeutics, the GRIN2B Foundation, the CureGRIN Foundation, and CombinedBrain. SFT is consultant for GRIN Therapeutics and Neurocrine, a cofounder of NeurOp, Inc. and Agrithera, and a member of the Board of Directors for NeurOp Inc. HY is the PI on a research grant from Sage Therapeutics to Emory and SJM is PI on a grant from GRIN Therapeutics to Emory. TAB – Consultancy for AveXis, Ovid, GW Pharmaceuticals, International Rett Syndrome Foundation, Takeda, Taysha, CureGRIN, GRIN Therapeutics, Alcyone, Neurogene, and Marinus; Clinical Trials with Acadia, Ovid, GW Pharmaceuticals, Marinus and RSRT; all remuneration has been made to his department.

Ethics approval This study was approved by the Medical Ethics Committee and the Institutional

Review Boards of University of Colorado School of Medicine and Children's Hospital Colorado (COMIRB 16-1520), Peking University First Hospital, John Hopkins University, Birmingham Women's and Children's Hospital, Emory University, and University of Leipzig Hospitals and Clinics. All in vitro studies were conducted according to the guidelines of Emory University.

References

1. Hansen KB, Wollmuth LP, Bowie D, Furukawa H, Menniti FS, Sobolevsky AI, Swanson GT, Swanger SA, Greger IH, Nakagawa T, McBain CJ, Jayaraman V, Low CM, Dell'Acqua ML, Diamond JS, Camp CR, Perszyk RE, Yuan H, Traynelis SF (2021) Structure, Function, and Pharmacology of Glutamate Receptor Ion Channels. Pharmacol Rev 73 (4):298-487. doi:10.1124/pharmrev.120.000131

2. Petrovski S, Wang Q, Heinzen EL, Allen AS, Goldstein DB (2013) Genic intolerance to functional variation and the interpretation of personal genomes. PLoS Genet 9 (8):e1003709. doi:10.1371/journal.pgen.1003709

3. de Ligt J, Willemsen MH, van Bon BW, Kleefstra T, Yntema HG, Kroes T, Vulto-van Silfhout AT, Koolen DA, de Vries P, Gilissen C, del Rosario M, Hoischen A, Scheffer H, de Vries BB, Brunner HG, Veltman JA, Vissers LE (2012) Diagnostic exome sequencing in persons with severe intellectual disability. N Engl J Med 367 (20):1921-1929. doi:10.1056/NEJMoa1206524

4. De Rubeis S, He X, Goldberg AP, Poultney CS, Samocha K, Cicek AE, Kou Y, Liu L, Fromer M, Walker S, Singh T, Klei L, Kosmicki J, Shih-Chen F, Aleksic B, Biscaldi M, Bolton PF, Brownfeld JM, Cai J, Campbell NG, Carracedo A, Chahrour MH, Chiocchetti AG, Coon H, Crawford EL, Curran SR, Dawson G, Duketis E, Fernandez BA, Gallagher L, Geller E, Guter SJ, Hill RS, Ionita-Laza J, Jimenz Gonzalez P, Kilpinen H, Klauck SM, Kolevzon A, Lee I, Lei I, Lei J, Lehtimaki T, Lin CF, Ma'ayan A, Marshall CR, McInnes AL, Neale B, Owen MJ, Ozaki N, Parellada M, Parr JR, Purcell S, Puura K, Rajagopalan D, Rehnstrom K, Reichenberg A, Sabo A, Sachse M, Sanders SJ, Schafer C, Schulte-Ruther M, Skuse D, Stevens C, Szatmari P, Tammimies K, Valladares O, Voran A, Li-San W, Weiss LA, Willsey AJ, Yu TW, Yuen RK, Study DDD, Homozygosity Mapping Collaborative for A, Consortium UK, Cook EH, Freitag CM, Gill M, Hultman CM, Lehner T, Palotie A, Schellenberg GD, Sklar P, State MW, Sutcliffe JS, Walsh CA, Scherer SW, Zwick ME, Barett JC, Cutler DJ, Roeder K, Devlin B, Daly MJ, Buxbaum JD (2014) Synaptic, transcriptional and chromatin genes disrupted in autism. Nature 515 (7526):209-215. doi:10.1038/nature13772

5. Geisheker MR, Heymann G, Wang T, Coe BP, Turner TN, Stessman HAF, Hoekzema K, Kvarnung M, Shaw M, Friend K, Liebelt J, Barnett C, Thompson EM, Haan E, Guo H, Anderlid BM, Nordgren A, Lindstrand A, Vandeweyer G, Alberti A, Avola E, Vinci M, Giusto S, Pramparo T, Pierce K, Nalabolu S, Michaelson JJ, Sedlacek Z, Santen GWE, Peeters H, Hakonarson H, Courchesne E, Romano C, Kooy RF, Bernier RA, Nordenskjold M, Gecz J, Xia K, Zweifel LS, Eichler EE (2017) Hotspots of missense mutation identify neurodevelopmental disorder genes and functional domains. Nat Neurosci 20 (8):1043-1051. doi:10.1038/nn.4589

6. Guo H, Duyzend MH, Coe BP, Baker C, Hoekzema K, Gerdts J, Turner TN, Zody MC, Beighley JS, Murali SC, Nelson BJ, University of Washington Center for Mendelian G, Bamshad MJ, Nickerson DA, Bernier RA, Eichler EE (2019) Genome sequencing identifies multiple deleterious variants in autism patients with more severe phenotypes. Genet Med 21 (7):1611-1620. doi:10.1038/s41436-018-0380-2

7. Ismail V, Zachariassen LG, Godwin A, Sahakian M, Ellard S, Stals KL, Baple E, Brown KT, Foulds N, Wheway G, Parker MO, Lyngby SM, Pedersen MG, Desir J, Bayat A, Musgaard M, Guille M, Kristensen AS, Baralle D (2022) Identification and functional evaluation of GRIA1 missense and truncation variants in individuals with ID: An emerging neurodevelopmental syndrome. American journal of human genetics 109 (7):1217-1241. doi:10.1016/j.ajhg.2022.05.009

8. Hamdan FF, Gauthier J, Araki Y, Lin DT, Yoshizawa Y, Higashi K, Park AR, Spiegelman D, Dobrzeniecka S, Piton A, Tomitori H, Daoud H, Massicotte C, Henrion E, Diallo O, Group SD, Shekarabi M, Marineau C, Shevell M, Maranda B, Mitchell G, Nadeau A, D'Anjou G, Vanasse M, Srour M, Lafreniere RG, Drapeau P, Lacaille JC, Kim E, Lee JR, Igarashi K, Huganir RL, Rouleau GA, Michaud JL (2011) Excess of de novo deleterious mutations in genes associated with glutamatergic systems in nonsyndromic intellectual disability. American journal of human genetics 88 (3):306-316. doi:10.1016/j.ajhg.2011.02.001

9. Salpietro V, Dixon CL, Guo H, Bello OD, Vandrovcova J, Efthymiou S, Maroofian R, Heimer G, Burglen L, Valence S, Torti E, Hacke M, Rankin J, Tariq H, Colin E, Procaccio V, Striano P, Mankad K, Lieb A, Chen S, Pisani L, Bettencourt C, Mannikko R, Manole A, Brusco A, Grosso E, Ferrero GB, Armstrong-Moron J, Gueden S, Bar-Yosef O, Tzadok M, Monaghan KG, Santiago-Sim T, Person RE, Cho MT, Willaert R, Yoo Y, Chae JH, Quan Y, Wu H, Wang T, Bernier RA, Xia K, Blesson A, Jain M, Motazacker MM, Jaeger B, Schneider AL, Boysen K, Muir AM, Myers CT, Gavrilova RH, Gunderson L, Schultz-Rogers L, Klee EW, Dyment D, Osmond M, Parellada M, Llorente C, Gonzalez-Penas J, Carracedo A, Van Haeringen A, Ruivenkamp C, Nava C, Heron D, Nardello R, Iacomino M, Minetti C, Skabar A, Fabretto A, Group SS, Raspall-Chaure M, Chez M, Tsai A, Fassi E, Shinawi M, Constantino JN, De Zorzi R, Fortuna S, Kok F, Keren B, Bonneau D, Choi M, Benzeev B, Zara F, Mefford HC, Scheffer IE, Clayton-Smith J, Macaya A, Rothman JE, Eichler EE, Kullmann DM, Houlden H (2019) AMPA receptor GluA2 subunit defects are a cause of neurodevelopmental disorders. Nature communications 10 (1):3094. doi:10.1038/s41467-019-10910-w

10. Alkelai A, Shohat S, Greenbaum L, Schechter T, Draiman B, Chitrit-Raveh E, Rienstein S, Dagaonkar N, Hughes D, Aggarwal VS, Heinzen EL, Shifman S, Goldstein DB, Kohn Y (2021) Expansion of the GRIA2 phenotypic representation: a novel de novo loss of function mutation in a case with childhood onset schizophrenia. Journal of human genetics 66 (3):339-343. doi:10.1038/s10038-020-00846-1

11. Zhou B, Zhang C, Zheng L, Wang Z, Chen X, Feng X, Zhang Q, Hao S, Wei L, Gu W, Hui L (2021) Case Report: A Novel De Novo Missense Mutation of the GRIA2 Gene in a Chinese Case of Neurodevelopmental Disorder With Language Impairment. Front Genet 12:794766. doi:10.3389/fgene.2021.794766

12. Wu Y, Arai AC, Rumbaugh G, Srivastava AK, Turner G, Hayashi T, Suzuki E, Jiang Y, Zhang L, Rodriguez J, Boyle J, Tarpey P, Raymond FL, Nevelsteen J, Froyen G, Stratton M, Futreal A, Gecz J, Stevenson R, Schwartz CE, Valle D, Huganir RL, Wang T (2007) Mutations in ionotropic AMPA receptor 3 alter channel properties and are associated with moderate cognitive impairment in humans. Proc Natl Acad Sci U S A 104 (46):18163-18168. doi:10.1073/pnas.0708699104

13. Philips AK, Siren A, Avela K, Somer M, Peippo M, Ahvenainen M, Doagu F, Arvio M, Kaariainen H, Van Esch H, Froyen G, Haas SA, Hu H, Kalscheuer VM, Jarvela I (2014) X-exome sequencing in Finnish families with intellectual disability--four novel mutations and two novel syndromic phenotypes. Orphanet J Rare Dis 9:49. doi:10.1186/1750-1172-9-49

14. Yang Y, Muzny DM, Xia F, Niu Z, Person R, Ding Y, Ward P, Braxton A, Wang M, Buhay C, Veeraraghavan N, Hawes A, Chiang T, Leduc M, Beuten J, Zhang J, He W, Scull J, Willis A, Landsverk M, Craigen WJ, Bekheirnia MR, Stray-Pedersen A, Liu P, Wen S, Alcaraz W, Cui H, Walkiewicz M, Reid J, Bainbridge M, Patel A, Boerwinkle E, Beaudet AL, Lupski JR, Plon SE, Gibbs RA, Eng CM (2014)

Molecular findings among patients referred for clinical whole-exome sequencing. JAMA 312 (18):1870-1879. doi:10.1001/jama.2014.14601

15. Davies B, Brown LA, Cais O, Watson J, Clayton AJ, Chang VT, Biggs D, Preece C, Hernandez-Pliego P, Krohn J, Bhomra A, Twigg SRF, Rimmer A, Kanapin A, Consortium WGS, Sen A, Zaiwalla Z, McVean G, Foster R, Donnelly P, Taylor JC, Blair E, Nutt D, Aricescu AR, Greger IH, Peirson SN, Flint J, Martin HC (2017) A point mutation in the ion conduction pore of AMPA receptor GRIA3 causes dramatically perturbed sleep patterns as well as intellectual disability. Human molecular genetics 26 (20):3869-3882. doi:10.1093/hmg/ddx270

16. Cherot E, Keren B, Dubourg C, Carre W, Fradin M, Lavillaureix A, Afenjar A, Burglen L, Whalen S, Charles P, Marey I, Heide S, Jacquette A, Heron D, Doummar D, Rodriguez D, Billette de Villemeur T, Moutard ML, Guet A, Xavier J, Perisse D, Cohen D, Demurger F, Quelin C, Depienne C, Odent S, Nava C, David V, Pasquier L, Mignot C (2018) Using medical exome sequencing to identify the causes of neurodevelopmental disorders: Experience of 2 clinical units and 216 patients. Clin Genet 93 (3):567-576. doi:10.1111/cge.13102

17. Piard J, Bereau M, XiangWei W, Wirth T, Amsallem D, Buisson L, Richard P, Liu N, Xu Y, Myers SJ, Traynelis SF, Chelly J, Anheim M, Raynaud M, Maldergem LV, Yuan H (2020) The GRIA3 c.2477G > A Variant Causes an Exaggerated Startle Reflex, Chorea, and Multifocal Myoclonus. Mov Disord 35 (7):1224-1232. doi:10.1002/mds.28058

18. Trivisano M, Santarone ME, Micalizzi A, Ferretti A, Dentici ML, Novelli A, Vigevano F, Specchio N (2020) GRIA3 missense mutation is cause of an x-linked developmental and epileptic encephalopathy. Seizure 82:1-6. doi:10.1016/j.seizure.2020.08.032

19. Sun JH, Chen J, Ayala Valenzuela FE, Brown C, Masser-Frye D, Jones M, Romero LP, Rinaldi B, Li WL, Li QQ, Wu D, Gerard B, Thorpe E, Bayat A, Shi YS (2021) X-linked neonatal-onset epileptic encephalopathy associated with a gain-of-function variant p.R660T in GRIA3. PLoS Genet 17 (6):e1009608. doi:10.1371/journal.pgen.1009608

20. Rinaldi B, Ge YH, Freri E, Tucci A, Granata T, Estienne M, Sun JH, Gerard B, Bayat A, Efthymiou S, Gervasini C, Shi YS, Houlden H, Marchisio P, Milani D (2022) Myoclonic status epilepticus and cerebellar hypoplasia associated with a novel variant in the GRIA3 gene. Neurogenetics 23 (1):27-35. doi:10.1007/s10048-021-00666-1

21. Hamanaka K, Miyoshi K, Sun JH, Hamada K, Komatsubara T, Saida K, Tsuchida N, Uchiyama Y, Fujita A, Mizuguchi T, Gerard B, Bayat A, Rinaldi B, Kato M, Tohyama J, Ogata K, Shi YS, Saito K, Miyatake S, Matsumoto N (2022) Amelioration of a neurodevelopmental disorder by carbamazepine in a case having a gain-of-function GRIA3 variant. Hum Genet 141 (2):283-293. doi:10.1007/s00439-021-02416-7

22. Martin S, Chamberlin A, Shinde DN, Hempel M, Strom TM, Schreiber A, Johannsen J, Ousager LB, Larsen MJ, Hansen LK, Fatemi A, Cohen JS, Lemke J, Sorensen KP, Helbig KL, Lessel D, Abou Jamra R (2017) De Novo Variants in GRIA4 Lead to Intellectual Disability with or without Seizures and Gait Abnormalities. American journal of human genetics 101 (6):1013-1020. doi:10.1016/j.ajhg.2017.11.004

23. Richards S, Aziz N, Bale S, Bick D, Das S, Gastier-Foster J, Grody WW, Hegde M, Lyon E, Spector E, Voelkerding K, Rehm HL, Committee ALQA (2015) Standards and guidelines for the interpretation of sequence variants: a joint consensus recommendation of the American College of Medical Genetics and

Genomics and the Association for Molecular Pathology. Genet Med 17 (5):405-424. doi:10.1038/gim.2015.30

24. Twomey EC, Yelshanskaya MV, Grassucci RA, Frank J, Sobolevsky AI (2017) Channel opening and gating mechanism in AMPA-subtype glutamate receptors. Nature 549 (7670):60-65. doi:10.1038/nature23479

25. Herguedas B, Garcia-Nafria J, Cais O, Fernandez-Leiro R, Krieger J, Ho H, Greger IH (2016) Structure and organization of heteromeric AMPA-type glutamate receptors. Science 352 (6285):aad3873. doi:10.1126/science.aad3873

26. Chen W, Tankovic A, Burger PB, Kusumoto H, Traynelis SF, Yuan H (2017) Functional Evaluation of a De Novo GRIN2A Mutation Identified in a Patient with Profound Global Developmental Delay and Refractory Epilepsy. Mol Pharmacol 91 (4):317-330. doi:10.1124/mol.116.106781

27. Stern-Bach Y, Russo S, Neuman M, Rosenmund C (1998) A point mutation in the glutamate binding site blocks desensitization of AMPA receptors. Neuron 21 (4):907-918. doi:10.1016/s0896-6273(00)80605-4

28. Hume RI, Dingledine R, Heinemann SF (1991) Identification of a site in glutamate receptor subunits that controls calcium permeability. Science 253 (5023):1028-1031. doi:10.1126/science.1653450

29. Verdoorn TA, Burnashev N, Monyer H, Seeburg PH, Sakmann B (1991) Structural determinants of ion flow through recombinant glutamate receptor channels. Science 252 (5013):1715-1718. doi:10.1126/science.1710829

30. Sommer B, Keinanen K, Verdoorn TA, Wisden W, Burnashev N, Herb A, Kohler M, Takagi T, Sakmann B, Seeburg PH (1990) Flip and flop: a cell-specific functional switch in glutamate-operated channels of the CNS. Science 249 (4976):1580-1585. doi:10.1126/science.1699275

31. Yuan H, Hansen KB, Zhang J, Pierson TM, Markello TC, Fajardo KV, Holloman CM, Golas G, Adams DR, Boerkoel CF, Gahl WA, Traynelis SF (2014) Functional analysis of a de novo GRIN2A missense mutation associated with early-onset epileptic encephalopathy. Nature communications 5:3251. doi:10.1038/ncomms4251

32. Chen C, Okayama H (1987) High-efficiency transformation of mammalian cells by plasmid DNA. Mol Cell Biol 7 (8):2745-2752. doi:10.1128/mcb.7.8.2745-2752.1987

33. Yuan H, Hansen KB, Vance KM, Ogden KK, Traynelis SF (2009) Control of NMDA receptor function by the NR2 subunit amino-terminal domain. J Neurosci 29 (39):12045-12058. doi:10.1523/JNEUROSCI.1365-09.2009

34. Swanger SA, Chen W, Wells G, Burger PB, Tankovic A, Bhattacharya S, Strong KL, Hu C, Kusumoto H, Zhang J, Adams DR, Millichap JJ, Petrovski S, Traynelis SF, Yuan H (2016) Mechanistic Insight into NMDA Receptor Dysregulation by Rare Variants in the GluN2A and GluN2B Agonist Binding Domains. American journal of human genetics 99 (6):1261-1280. doi:10.1016/j.ajhg.2016.10.002

35. Perszyk RE, Kristensen AS, Lyuboslavsky P, Traynelis SF (2021) Three-dimensional missense tolerance ratio analysis. Genome research 31 (8):1447-+. doi:10.1101/gr.275528.121

36. Twomey EC, Yelshanskaya MV, Sobolevsky AI (2019) Structural and functional insights into transmembrane AMPA receptor regulatory protein complexes. Journal of General Physiology 151 (12):1347-1356. doi:10.1085/jgp.201812264

37. Colquhoun D (1998) Binding, gating, affinity and efficacy: the interpretation of structure-activity relationships for agonists and of the effects of mutating receptors. Br J Pharmacol 125 (5):924-947. doi:10.1038/sj.bjp.0702164

38. Trussell LO, Zhang S, Raman IM (1993) Desensitization of AMPA receptors upon multiquantal neurotransmitter release. Neuron 10 (6):1185-1196. doi:10.1016/0896-6273(93)90066-z

39. Myers SJ, Yuan H, Perszyk RE, Zhang J, Kim S, Nocilla KA, Allen JP, Bain JM, Lemke JR, Lal D, Benke TA, Traynelis SF (2023) Classification of missense variants in the N-methyl-D-aspartate receptor GRIN gene family as gain- or loss-of-function. Human molecular genetics. doi:10.1093/hmg/ddad104

40. Rosenmund C, Stern-Bach Y, Stevens CF (1998) The tetrameric structure of a glutamate receptor channel. Science 280 (5369):1596-1599. doi:10.1126/science.280.5369.1596

41. Kristensen AS, Jenkins MA, Banke TG, Schousboe A, Makino Y, Johnson RC, Huganir R, Traynelis SF (2011) Mechanism of Ca2+/calmodulin-dependent kinase II regulation of AMPA receptor gating. Nat Neurosci 14 (6):727-735. doi:10.1038/nn.2804

42. De Liso P, Moavero R, Coppola G, Curatolo P, Cusmai R, De Sarro G, Franzoni E, Vigevano F, Verrotti A (2017) Current role of perampanel in pediatric epilepsy. Ital J Pediatr 43 (1):51. doi:10.1186/s13052-017-0368-6

43. Swiderska N, Tan HJ, Rajai A, Silwal A, Desurkar A, Martland T (2017) Effectiveness and tolerability of Perampanel in children, adolescents and young adults with refractory epilepsy: A UK national multicentre study. Seizure 52:63-70. doi:10.1016/j.seizure.2017.08.014

44. Lim GY, Chen CL, Chan Wei Shih D (2021) Utility and Safety of Perampanel in Pediatric FIRES and Other Drug-Resistant Epilepsies. Child Neurol Open 8:2329048X211055335. doi:10.1177/2329048X211055335

45. Coombs ID, Ziobro J, Krotov V, Surtees TL, Cull-Candy SG, Farrant M (2022) A gain-of-function GRIA2 variant associated with neurodevelopmental delay and seizures: Functional characterization and targeted treatment. Epilepsia 63 (12):e156-e163. doi:10.1111/epi.17419

46. Singh T, Poterba T, Curtis D, Akil H, Al Eissa M, Barchas JD, Bass N, Bigdeli TB, Breen G, Bromet EJ, Buckley PF, Bunney WE, Bybjerg-Grauholm J, Byerley WF, Chapman SB, Chen WJ, Churchhouse C, Craddock N, Cusick CM, DeLisi L, Dodge S, Escamilla MA, Eskelinen S, Fanous AH, Faraone SV, Fiorentino A, Francioli L, Gabriel SB, Gage D, Gagliano Taliun SA, Ganna A, Genovese G, Glahn DC, Grove J, Hall MH, Hamalainen E, Heyne HO, Holi M, Hougaard DM, Howrigan DP, Huang H, Hwu HG, Kahn RS, Kang HM, Karczewski KJ, Kirov G, Knowles JA, Lee FS, Lehrer DS, Lescai F, Malaspina D, Marder SR, McCarroll SA, McIntosh AM, Medeiros H, Milani L, Morley CP, Morris DW, Mortensen PB, Myers RM, Nordentoft M, O'Brien NL, Olivares AM, Ongur D, Ouwehand WH, Palmer DS, Paunio T, Quested D, Rapaport MH, Rees E, Rollins B, Satterstrom FK, Schatzberg A, Scolnick E, Scott LJ, Sharp SI, Sklar P, Smoller JW, Sobell JL, Solomonson M, Stahl EA, Stevens CR, Suvisaari J, Tiao G, Watson SJ, Watts NA, Blackwood DH, Borglum AD, Cohen BM, Corvin AP, Esko T, Freimer NB, Glatt SJ, Hultman CM, McQuillin A, Palotie A, Pato CN, Pato MT, Pulver AE, St Clair D, Tsuang MT, Vawter MP, Walters JT, Werge TM, Ophoff RA, Sullivan PF, Owen MJ, Boehnke M, O'Donovan MC, Neale BM, Daly MJ (2022) Rare coding variants in ten genes confer substantial risk for schizophrenia. Nature 604 (7906):509-516. doi:10.1038/s41586-022-04556-w

Table 1. Summary of variant and patient information

#	Gene	Genotype	Protein	Location	#gnomAD	Inheritance	Phenotypes	Source
1	*GRIA1*	c.1568G>A	p.Gly523Glu	ABD (S1)	0	*de novo*	Epi, ID	this study
2	*GRIA1*	c.1906G>A	p.AlaA636Thr	M3	0	*de novo*	ID, ASD, hypotonias	a, b, c, d, this study
3	*GRIA1*	c.1988C>T	p.Thr663Met	ABD (S2)	0		not specified	a
4	*GRIA1*	c.2234G>A	p.Gly745Asp	ABD (S2)	0		ASD, ID	a, e
5	*GRIA1*	c.2645G>C	p.Ser882Thr	CTD	0	*de novo*	Epi, ID	this study
6	*GRIA2*	c.1523A>T	p.Glu508Val	ABD (S1)	0		Epi	this study
7	*GRIA2*	c.1760A>C	p.Glu587Ala	M1-M2 Link	0		not specified	this Study
8	*GRIA2*	c.1831G>A	p.Asp611Asn	M2	0		ASD, ID, Tourette's, aggression, language impairment	a, f, this study
9	*GRIA2*	c.1859G>A	p.Arg620His	M2-M3 link	0	*de novo*	Epi, ID	this study
10	*GRIA2*	c.1940T>C	p.Val647Ala	M2-M3 link	0	*de novo*	Epi, ID	this study
11	*GRIA2*	c.1939G>C	p.Val647Leu	M2-M3 link	0	*de novo*	Epi, ID, language impairment, behavioral abnormalities	a, f, this study
12	*GRIA2*	c.2341G>C	p.Asp781His	Pre-M4	0		ID	g
13	*GRIA3*	c.106A>G	p.Ile36Val	SP	5/204240		Epi, ID	a, this study
14	*GRIA3*	c.159T>G	p.Phe53Leu	NTD	0		Inborn genetic disease	a
15	*GRIA3*	c.783G>A	p.Met261Ile	NTD	3/183409		Epi, ID	this study
16	*GRIA3*	c.1010C>G	p.Ala337Gly	NTD	1/182814		Epi, ID	a, this study
17	*GRIA3*	c.1349G>A	p.Arg450Gln	ABD (S1)	6/204972		Epi, ID	a, h, this study
18	*GRIA3*	c.1502G>C	p.Arg501Thr	ABD (S1)	0		Epi, ID, dysphagia	a
19	*GRIA3*	c.1531A>G	p.Ile511Val	ABD (S1)	0		not specified	this study
20	*GRIA3*	c.1581C>A	p.Ser527Arg	ABD (S1)	0		Epi, ID, macrocephaly	this study
21	*GRIA3*	c.1679T>C	p.Val560Ala	M1	0		Epi, ID	this study
22	*GRIA3*	c.1701C>A	p.Ser567Arg	M1	0		not specified	a
23	*GRIA3*	c.1755CAA	p.Asn587del	M1-M2 Link	0		not specified	a
24	*GRIA3*	c.1850T>C	p.Met617Thr	M2	0		History of neurodevelopmental disorder	a
25	*GRIA3*	c.1888G>C, G>A	p.Gly630Arg	M2-M3 link	0		Epi, ID, autistic features, short stature, behavioral problems	a, i
26	*GRIA3*	c.1891C>A	p.Arg631Ser	M2-M3 link	0		Epi, ID	a, h
27	*GRIA3*	c.1940C>T	p.Ser647Phe	M3	0		Inborn genetic disease	a
28	*GRIA3*	c.1957G>T	p.Ala653Ser	M3	0	*de novo*	Epi, ID	this study
29	*GRIA3*	c.1957G>A	p.Ala653Thr	M3	0		ID, sleep disorder	a, j
30	*GRIA3*	c.1964T>C	p.Phe655Ser	M3	0		ID, hypotonia	a, k
31	*GRIA3*	c.1973T>C	p.Val658Ala	M3-S2 link	0	*de novo*	Epi, ID	this study
32	*GRIA3*	c.1980G>C	p.Arg660Ser	M3-S2 link	0		Inborn genetic disease	a
33	*GRIA3*	c.1991C>T	p.Pro664Leu	M3-S2 link	0		not specified	a
34	*GRIA3*	c.2116A>C	p.Met706Leu	ABD (S2)	0		Epi, ID, hypotonia, dysmorphisms, structural brain abnormalities, myopia	a, l
35	*GRIA3*	c.2117T>C	p.Met706Thr	ABD (S2)	0		ID, asthenic body habitus, poor muscle bulk, distal muscle weakness, hyporeflexia	a
36	*GRIA3*	c.2219T>C	p.Met740Thr	ABD (S2)	0		History of neurodevelopmental disorder	a
37	*GRIA3*	c.2321T>C	p.Leu774Ser	ABD (S2)	0		Inborn genetic disease	a
38	*GRIA3*	c.2327C>T	p.Thr776Met	ABD (S2)	0		Epi, epileptic encephalopathy, ID	a, this study
39	*GRIA3*	c.2408G>A	p.Gly803Glu	ABD (S2)	0		ID, tremors, spasticity, hyperekplexia, failure to thrive, microcephaly/dysmorphic ears	a
40	*GRIA3*	c.2416G>A	p.Gly806Ser	ABD (S2)	0		not specified	a
41	*GRIA3*	c.2447C>T	p.Thr816Ile	Pre-M4	0		Epi, ID, aggressive behavior	a
42	*GRIA3*	c.2452G>A	p.Ala818Thr	Pre-M4	0		not specified	a
43	*GRIA3*	c.2470G>A	p.Val824Met	M4	0		not specified	a
44	*GRIA3*	c.2477G>A	p.Gly826Asp	M4	0		ID, dysarthria, movement disorders	m
45	*GRIA3*	c.2497G>A	p.Gly833Arg	M4	0		ASD, Epi, ID, macrocephaly, myoclonic jerks	a, h
46	*GRIA4*	c.1162G>C	p.Gly388Arg	NTD	0	ND*	Epi, ID	this study
47	*GRIA4*	c.1915A>T	p.Thr639Ser	M3	0	*de novo*	Epi, ID, gait abnormality	a, n
48	*GRIA4*	c.1921A>G	p.Asn641Asp	M3	0	*de novo*	Epi, ID	a, n
49	*GRIA4*	c.1928C>G	p.Ala643Gly	M3	0	*de novo*	Epi, ID	a, n
50	*GRIA4*	c.1931C>T	p.Ala644Val	M3	0	*de novo*	Epi, ID	a, n
51	*GRIA4*	c.2090G>C	p.Arg697Pro	ABD (S2)	0	*de novo*	ID	a, n
52	*GRIA4*	c.2090G>A	p.Arg697Gln	ABD (S2)	4/248092		not specified	this study

ASD: autistic spectrum disorder, Epi: epilepsy, ID: intellectual disability; ND*: not determined, not maternally inherited (paternal sample unavailable)
a: ClinVar; b: de Ligt et al., 2012; c: De Rubeis et al., 2014; d: Geisheker et al., 2017; e: Guo et al., 2019; f: Salpietro et al., 2019; g: Hamdan et al., 2011; h: Wu et al., 2007; i: Philips et al., 2014; j: Davie et al., 2017; k: Chéro et al., 2018; l: Yang et al., 2014; m: Piard et al., 2020; n: Martin et al., 2017

Table 2. Summary of agonist potency and surface expression

Variant	Location	Glu EC_{50}, μM	KA EC_{50}, μM	Surface/total%	Total%
WT A1	--	7.2 ± 0.8 (14)	no response[b] (32)	100 (5)	100 (5)
A1-G523E	ABD (S1)	7.0 ± 1.2 (11)	no response[b] (32)	18 ± 6.6 (4)*	85 ± 6.3 (4)
A1-A636T	M3	1.1 ± 0.1 (17)*	no response[b] (22)	70 ± 6.4 (4)	110 ± 23 (4)
A1-T663M	ABD (S2)	38 ± 3.4 (16)*	no response[b] (28)	71 ± 6.9 (4)	85 ± 11 (4)
A1-G745D	ABD (S2)	no response[a] (18)	no response[b] (22)	38 ± 10 (5)*	84 ± 7.3 (5)
A1-S882T	CTD	9.4 ± 1.8 (17)	no response[b] (20)	108 ± 13 (4)	95 ± 19 (4)
WT A2	--	9.9 ± 0.9 (17)	92 ± 11 (13)	100 (6)	100 (6)
A2-E508V	ABD (S1)	6.6 ± 1.0 (15)*	180 ± 23 (12)*	22 ± 6.7 (5)*	60 ± 13 (5)*
A2-E587A	M1-M2 Link	8.3 ± 1.0 (14)	128 ± 8.1 (14)	128 ± 4.0 (4)	111 ± 4.7 (4)
A2-D611N	M2	9.4 ± 1.4 (13)	135 ± 14 (12)	99 ± 7.8 (4)	111 ± 8.0 (4)
A2-R620H	M2-M3 link	no response[a] (10)	no response[b] (12)	99 ± 4.0 (5)	94 ± 8.1 (5)
A2-V647A	M2-M3 link	4.4 ± 0.5 (11)*	57 ± 10 (12)	52 ± 6.7 (4)*	84 ± 8.2 (4)
A2-V647L	M2-M3 link	4.7 ± 0.5 (12)*	104 ± 12 (14)	45 ± 5.2 (4)*	52 ± 9.3 (4)*
A2-D781H [c]	Pre-M4	14 ± 2.0 (14)	97 ± 15 (11)	70 ± 16 (6)	57 ± 14 (6)*
WT A3	--	47 ± 0.3 (78)	164 ± 14 (36)	100 (19)	100 (19)
A3-I36V	SP	37 ± 1.8 (16)	126 ± 3.5 (12)	48 ± 9.7 (4)*	67 ± 5.7 (4)
A3-F53L	NTD	58 ± 2.2 (12)	179 ± 10 (15)	NA	NA
A3-M261I	NTD	36 ± 3.6 (19)	134 ± 4.6 (12)	38 ± 5.6 (4)*	44 ± 4.4 (4)*
A3-A337G	NTD	50 ± 3.4 (22)	140 ± 3.0 (12)	49 ± 3.3 (4)*	61 ± 11 (4)
A3-R450Q	ABD (S1)	36 ± 1.4 (19)	116 ± 2.2 (12)*	4.5 ± 6.0 (7)*	19 ± 7.4 (7)*
A3-R501T	ABD (S1)	30 ± 1.0 (12)	158 ± 7.9 (13)	17 ± 5.1 (4)*	43 ± 11 (4)*
A3-I511V	ABD (S1)	no response[a] (22)	120 ± 6.9 (11)	8.3 ± 2.6 (4)*	33 ± 10 (4)*
A3-S527R	ABD (S1)	21 ± 1.4 (18)*	no response[b] (10)	31 ± 8.1 (4)*	35 ± 6.6 (4)*
A3-V560A	M1	28 ± 2.5 (15)*	131 ± 4.7 (13)	58 ± 6.8 (4)*	22 ± 11 (4)*
A3-S567R	M1	no response[a] (18)	no response[b] (12)	21 ± 7.3 (4)*	19 ± 5.3 (4)*
A3-N587del	M1-M2 Link	52 ± 2.2 (12)	173 ± 6.2 (14)	27 ± 13 (4)*	43 ± 16 (4)*
A3-M617T	M2	119 ± 9.4 (12)*	no response[b] (10)	53 ± 9.8 (4)*	47 ± 7.6 (4)*
A3-G630R	M2-M3 link	no response[a] (12)	no response[b] (10)	59 ± 7.6 (5)*	105 ± 24 (5)
A3-R631S	M2-M3 link	no response[a] (12)	no response[b] (12)	42 ± 14 (5)*	70 ± 18 (5)
A3-S647F	M3	29 ± 1.8 (14)*	129 ± 9.2 (14)	43 ± 12 (5)*	51 ± 10 (5)*
A3-A653S	M3	18 ± 1.8 (18)*	58 ± 4.8 (13)*	48 ± 9.0 (4)*	47 ± 4.6 (4)*
A3-A653T	M3	70 ± 6.6 (18)*	no response[b] (10)	94 ± 6.3 (4)	62 ± 5.9 (4)
A3-F655S	M3	185 ± 15 (13)*	no response[b] (10)	56 ± 7.5 (4)*	78 ± 15 (4)
A3-V658A	M3-S2 link	21 ± 3.1 (12)*	56 ± 5.0 (12)*	41 ± 5.5 (4)*	83 ± 8.6 (4)
A3-R660S	M3-S2 link	15 ± 1.4 (30)*	78 ± 5.1 (15)*	29 ± 8.5 (5)*	42 ± 15 (5)*
A3-P664L	M3-S2 link	58 ± 7.7 (14)	201 ± 14 (18)*	5.7 ± 2.5 (4)*	3.6 ± 1.1 (4)*
A3-M706L	ABD (S2)	31 ± 1.2 (13)	272 ± 10 (16)*	40 ± 11 (5)*	45 ± 15 (5)*
A3-M706T	ABD (S2)	344 ± 32 (18)*	no response[b] (10)	41 ± 7.4 (4)*	61 ± 9.4 (4)
A3-M740T	ABD (S2)	46 ± 4.5 (17)	361 ± 7.7 (17)*	52 ± 12 (5)*	20 ± 5.5 (5)*
A3-L774S [c]	ABD (S2)	68 ± 2.5 (12)*	226 ± 13 (14)*	16 ± 10 (5)*	24 ± 8.1 (5)*
A3-T776M [d]	ABD (S2)	52 ± 2.4 (14)	193 ± 3.5 (16)*	44 ± 6.1 (4)*	68 ± 9.3 (4)
A3-G803E [c]	ABD (S2)	1.3 ± 0.2 (11)*	13 ± 1.0 (14)*	50 ± 10 (4)*	83 ± 8.6 (4)
A3-G806S [c]	ABD (S2)	103 ± 5.8 (16)*	314 ± 11 (13)*	50 ± 13 (5)*	32 ± 5.0 (5)*
A3-T816I [c]	Pre-M4	118 ± 6.4 (12)*	96 ± 7.0 (15)*	59 ± 9.6 (4)*	51 ± 14 (4)*
A3-A818T [c]	Pre-M4	9.9 ± 1.2 (11)*	111 ± 6.2 (8)*	23 ± 9.4 (5)*	28 ± 16 (5)*
A3-V824M	M4	56 ± 3.2 (16)	no response[b] (12)	55 ± 16 (5)*	43 ± 17 (5)*
A3-G826D	M4	36 ± 3.8 (17)	no response[b] (12)	18 ± 4.4 (4)*	42 ± 6.4 (4)*
A3-G833R	M4	no response[a] (12)	no response[b] (12)	25 ± 1.2 (4)*	53 ± 13 (4)*
WT A4	--	55 ± 3.6 (62)	113 ± 5.5 (24)	100 (7)	100 (7)
A4-G388R	NTD	no response[a] (8)	no response[b] (14)	6.9 ± 5.4 (4)*	89 ± 3.5 (4)
A4-T639S	M3	5.3 ± 0.7 (27)*	29 ± 2.4 (19)*	72 ± 6.4 (6)*	95 ± 9.2 (6)
A4-N641D	M3	4.8 ± 0.3 (13)*	13 ± 0.9 (12)*	1.6 ± 3.7 (5)*	3.3 ± 1.7 (5)*
A4-A643G	M3	1.8 ± 0.3 (12)*	12 ± 1.4 (12)*	57 ± 3.3 (4)*	91 ± 4.5 (4)
A4-A644V	M3	9.1 ± 1.9 (19)*	8.5 ± 0.6 (15)*	101 ± 8.0 (4)	83 ± 7.6 (4)
A4-R697P	ABD (S2)	241 ± 13 (19)*	82 ± 4.7 (11)*	9.8 ± 2.5 (4)*	36 ± 13 (4)*
A4-R697Q	ABD (S2)	89 ± 5.2 (17)*	139 ± 5.7 (13)	87 ± 11 (4)	68 ± 13 (4)*

Data are mean SEM (n). *p<0.05, one-way ANOVA; NA: not available. [a] no current at 3 mM glutamate. [b] no current at 3 mM kainate. [c] Located in conserved region shared by both flip and flop splice variants; [d] only present in the flip alternative splice cassette.

FIGURE LEGENDS

Fig. 1. EEG features and brain MRI for patients with *GRIA* variants. ***(A)*** EEG of Patient-4 (*GRIA3*-p.Ala653Ser) (Table 1; Supplemental Table S1) shows multiple spikes, spike-wave and waves predominately in right lobe (asterisks; 2-year-old). ***(B)*** The EEG of the Patient-5 (*GRIA3*-p.Val658Ala) (Table 1; Supplemental Table S1) indicates multiple spike and spike-wave complex in the left parieto-temporo-occipital region region predominately during sleep (5-year-old). ***(C)*** The EEG of the Patient-10 (*GRIA4*-p.Gly388Arg) (Table 1; Supplemental Table S1) at age 9 reveals multiple spike-waves that are activated by sleep and are present on the right (temporal, parietal and central regions) extending to the left central region. ***(D)*** T2-weighted MRI of the patient with *GRIA4*-p.Asn641Asp variant (Table 1) at age 15 demonstrates severe microcephaly with significantly decreased volume of bilateral frontal lobes with enlarged lateral ventricles and subarachnoid spaces, including bilateral sylvian fissures. The posterior fossa (not shown) and basal ganglia appeared normal; there was no change in myelination.

Fig. 2. Location of *GRIA1-4* variants in / GluA1-4 in comparison to their 3DMTR. (***A***) Ribbon structure of the open GluA2 receptor (PDB:5WEO, [24]). (***B***) A view of the isolated chain A showing the semi-autonomous domains; NTD in *blue*, ABD-S1 in *pink*, ABD-S2 in *purple*, and TMD in *green*). (***C***) Linear raster plots of the *GRIA1-4* residues (present in the structure used) depicting the 3DMTR (*blue* depicts more intolerant residues, *red* depicts more tolerant residues, with the scale shown in the *bottom left* of panel B), the *de novo* variants (*purple*), gnomAD missense variants (*orange*), and gnomAD synonymous variants (*green*). *See* Supplemental Fig. S1 for a plot of the 3DMTR data. The subunit domains are depicted on the same linear x-scale at the *bottom* of the panel. Note that GluA3 3DMTR score is slightly more volatile due to being X-linked.

Fig. 3. Structural representation of GluA1-4 receptor 3DMTR scores. (***A***) The 3DMTR scores of GluA1-4 are shown, chain A using the same view as depicted in Figure 2 (*see* Supplemental Information for annotated pdb files). The scale bar is shown in the *top left*, with more intolerant residues shown in *blue* and more tolerant residues shown in *red*. Salient differences in the 3DMTR scores of each *GRIA* gene are marked. M1 and M4 are sites for interaction with auxiliary subunits such as TARPs, GSG1L, and cornichon proteins [1]. (***B***) Intolerant regions of the GluA1-4 receptor NTD**.** Surface representation of the NTD of the GluA2 receptor model, highlighting one NTD dimer (Chain A and Chain B colored as in Figure 2). The same scale bar is used as in ***A***. *See* Supplemental Fig. S3 for an alternative 3DMTR score for GluA3 using the GluA2/GluA3 heteromeric receptor structure. A 3DMTR structural file with intolerance color-coded is available for all *GRIA* genes as Supplemental Material.

Fig. 4. Variant GluA1-4 receptors show altered pharmacological properties. (***A***-***D***) Composite concentration-response curves for glutamate recorded at a V_{HOLD} of -40 mV for GluA1 **(*A*)**, GluA2 **(*B*)**, GluA3 **(*C*)**, GluA4 **(*D*)** homomeric AMPARs. GluA3 was co-expressed with human stargazin to increase response amplitude. Smooth curves are *Equation 1* fitted to the data. Data in all composite concentration-response curves are mean ± SEM.

Fig. 5. Variant GluA1-4 receptors change response time course and cell surface expression. (***A***) Representative whole cell voltage clamp current recordings are shown in response to application of 10 mM glutamate for a duration of 100 ms (represented by open bar on the top of traces) from HEK293 cells transfected with cDNA encoding WT GluA4, GluA4-T639S, GluA4-A643G and

GluA4-A644V. (***B-E***) Representative plots of nitrocefin absorbance (O.D.) versus time (*Left panels*) are shown for HEK293 cells expressing WT or mutant GluAs. WT GluA2 and the TARP gamma-2 were present with WT or mutant β-lac-GluA3 in all conditions. (*Right panels*) The slopes of O.D. versus time were averaged (n = 4 - 19 independent experiments) and plotted as percentages of WT for the ratio of surface/total. Data in all bar graphs (*Right panels*) are mean ± SEM. Data were analyzed by one-way ANOVA with Dunnett's Multiple Comparison Test compared to WT (surface/total ratio, *$p < 0.05$, **$p < 0.01$, ***$p < 0.001$).

Fig. 6. Effects of AMPAR positive or negative modulators on WT and variant AMPARs. (***A-H***) Summary of the degree of potentiation, normalized to the agonist-evoked current amplitude from two electrode voltage clamp recordings from *Xenopus* oocytes in the presence of 1000 μM kainic acid at holding potential of -40 to -60 mV. Human stargazin (γ-2) was co-injected with WT and mutant GluA3. (***A***) CX-614, (***B***) anirecetam, (***C***) cyclothiazide, (***D***) CP-465022, (***E***) perampanel, (***F***) GYKI52466, (***G***) GYKI53655, and (***H***) NBQX. (***I-L***) Composite concentration-response curves of AMPAR positive or negative modulators were evaluated by two electrode voltage clamp recordings from *Xenopus oocytes* in the presence of 1000 μM kainic acid at a holding potential of -40 to -60 mV. (***I-J***) CP465022, and (***K-L***) perampanel. (***M-N***) Concentration-response curves of kainic acid on WT GluA4 and GluA4-R697P were recorded in the absence and presence of CX-614. Data in all bar graphs (***A-H***) are mean ± 95% CI (confidence interval). Data in all composite concentration-response curves (***I-N***) are mean ± SEM. Smooth curves are *Equation 2* fitted to the data. *See* Supplemental Tables S3, S4, S5 for a summary of fitted parameters and quantitative analysis.

Figure-1

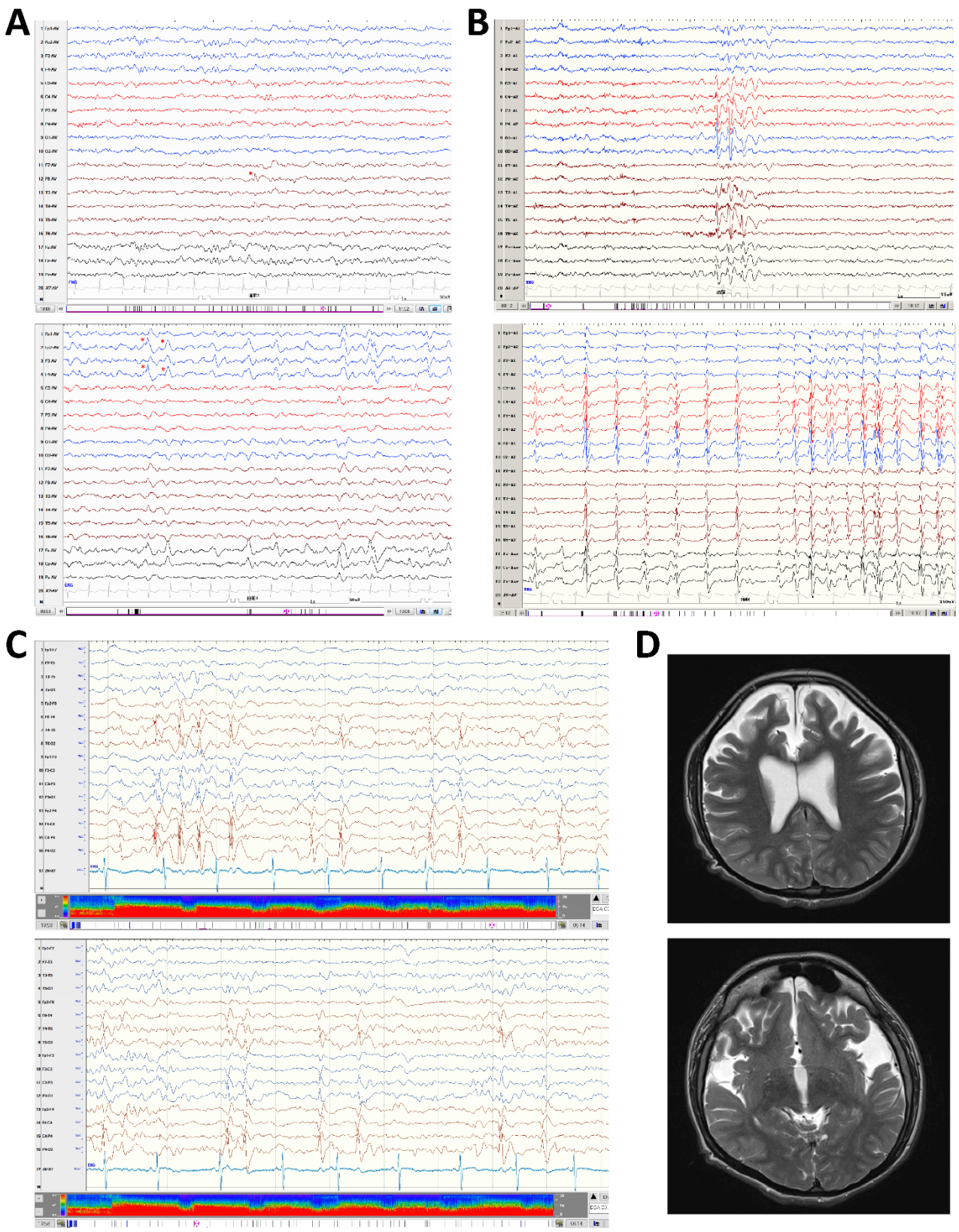

Figure-2

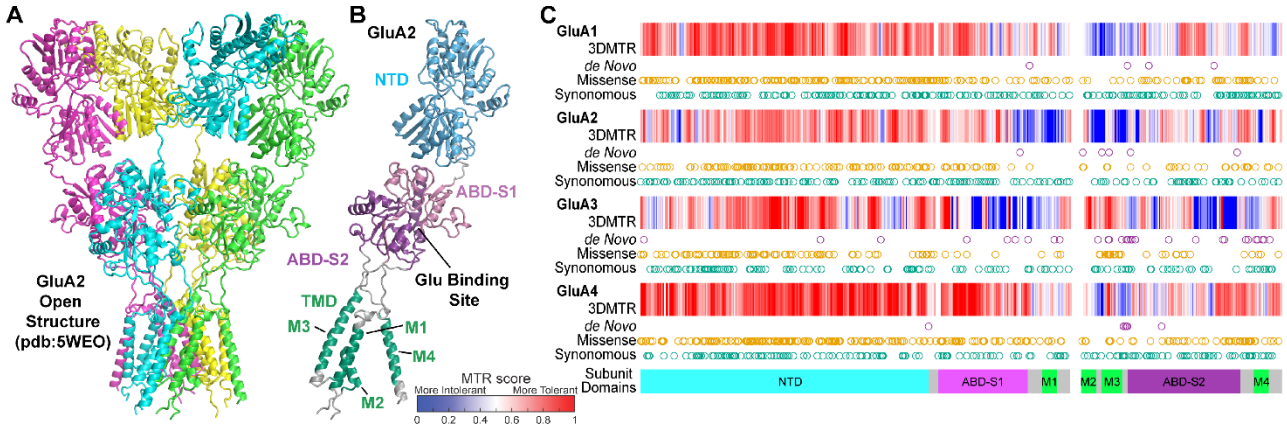
A
GluA2
Open
Structure
(pdb:5WEO)
B
GluA2
NTD
ABD-S1
ABD-S2
Glu Binding
Site
TMD
M3
M1
M4
M2
MTR score
More Intolerant
More Tolerant
0
0.2
0.4
0.6
0.8
1
C
GluA1
3DMTR
de Novo
Missense
Synonomous
GluA2
3DMTR
de Novo
Missense
Synonomous
GluA3
3DMTR
de Novo
Missense
Synonomous
GluA4
3DMTR
de Novo
Missense
Synonomous
Subunit
Domains
NTD
ABD-S1
M1
M2
M3
ABD-S2
M4

Figure-3

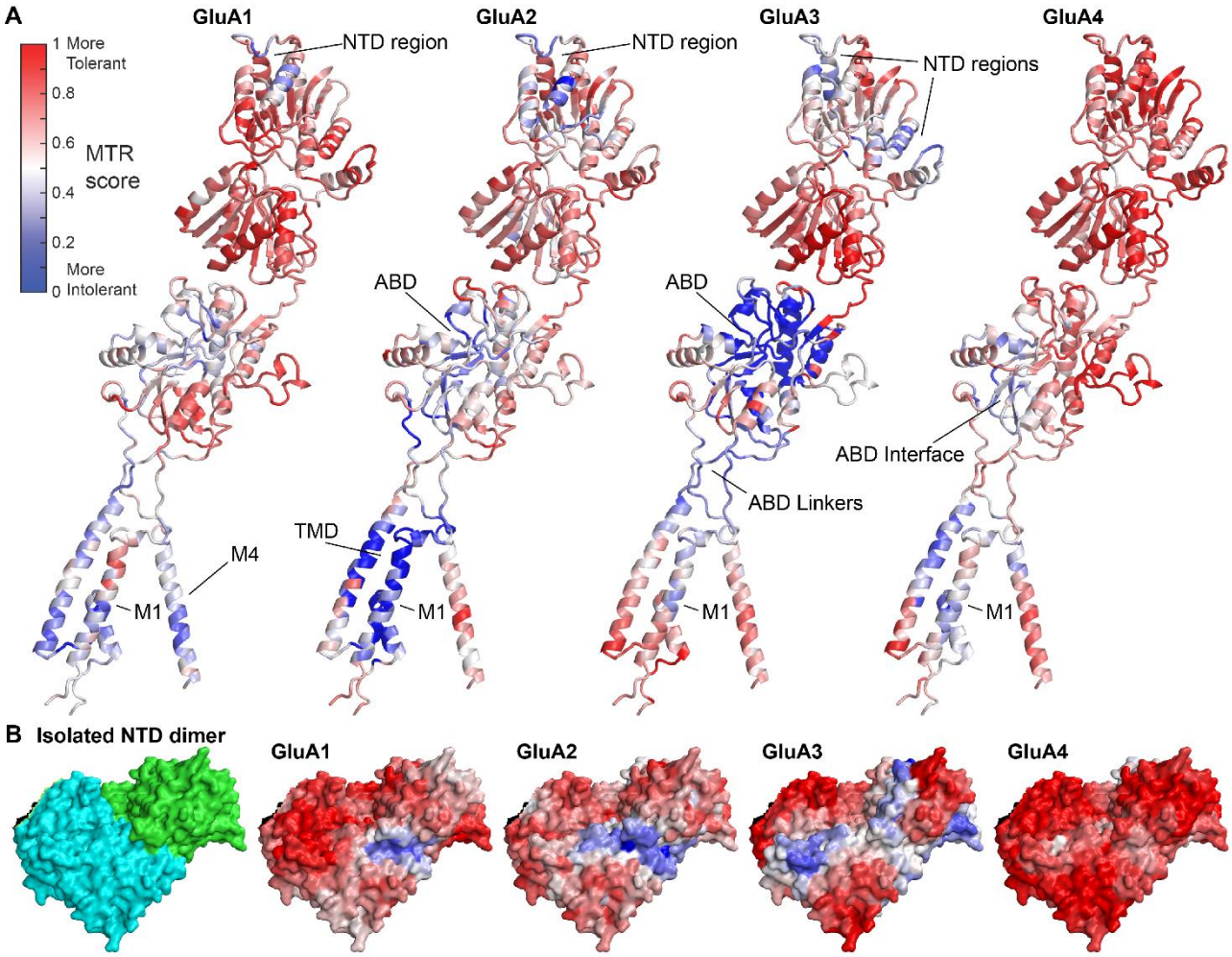
A
GluA1
GluA2
GluA3
GluA4
1 More Tolerant
0.8
0.6
MTR score
0.4
0.2
More Intolerant
0
NTD region
NTD region
NTD regions
ABD
ABD
ABD Interface
ABD Linkers
TMD
M4
M1
M1
M1
M1
B Isolated NTD dimer
GluA1
GluA2
GluA3
GluA4

Figure-4

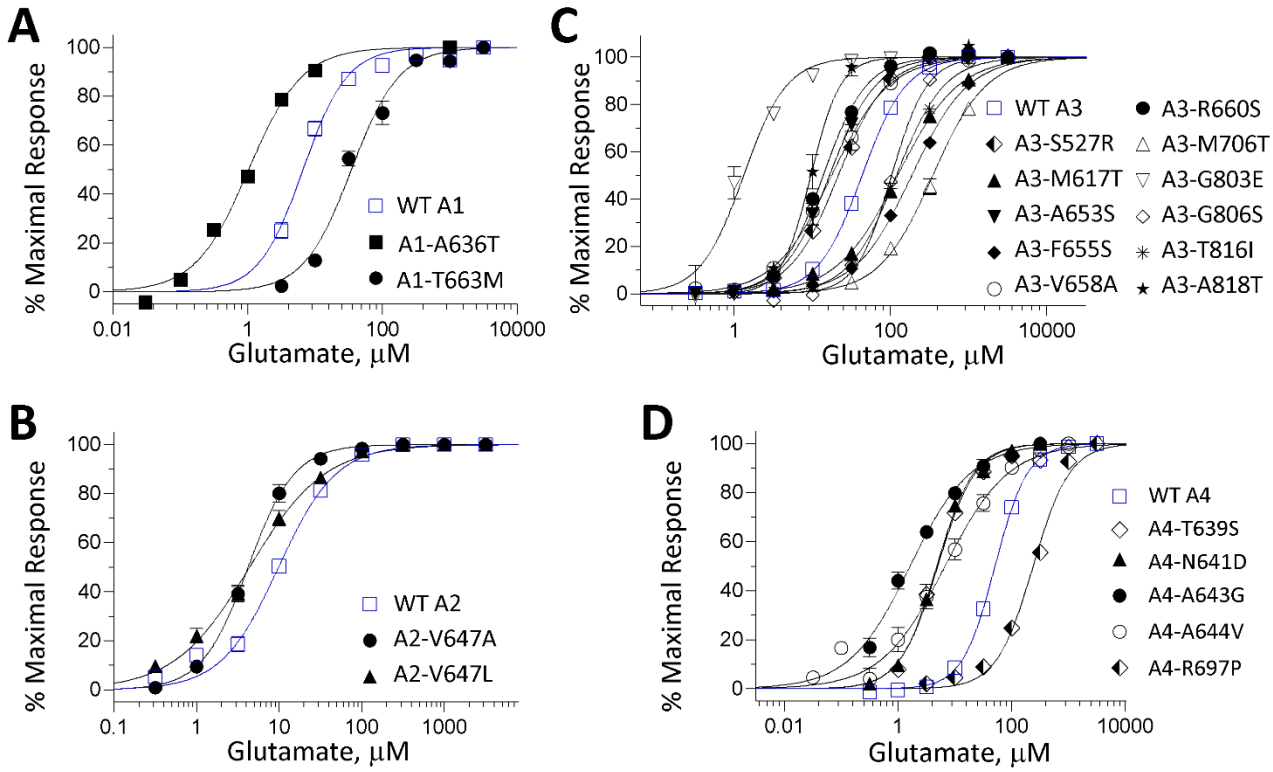
A
% Maximal Response
Glutamate, μM
WT A1
A1-A636T
A1-T663M
B
% Maximal Response
Glutamate, μM
WT A2
A2-V647A
A2-V647L
C
% Maximal Response
Glutamate, μM
WT A3
A3-S527R
A3-M617T
A3-A653S
A3-F655S
A3-V658A
A3-R660S
A3-M706T
A3-G803E
A3-G806S
A3-T816I
A3-A818T
D
% Maximal Response
Glutamate, μM
WT A4
A4-T639S
A4-N641D
A4-A643G
A4-A644V
A4-R697P

Figure-5

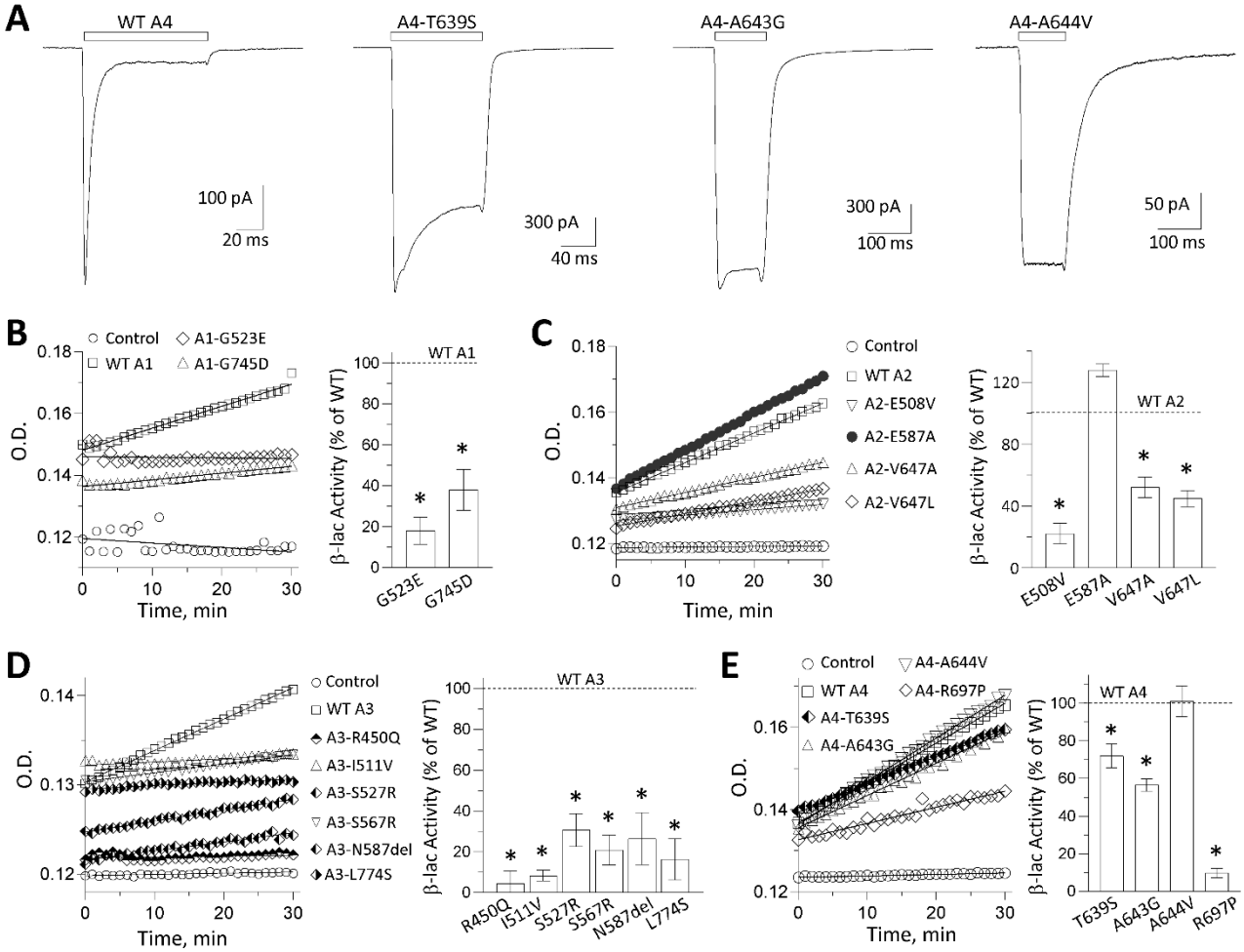
A
WT A4
A4-T639S
A4-A643G
A4-A644V
100 pA
20 ms
300 pA
40 ms
300 pA
100 ms
50 pA
100 ms
B
Control
A1-G523E
WT A1
A1-G745D
O.D.
Time, min
β-lac Activity (% of WT)
WT A1
G523E
G745D
C
Control
WT A2
A2-E508V
A2-E587A
A2-V647A
A2-V647L
O.D.
Time, min
β-lac Activity (% of WT)
WT A2
E508V
E587A
V647A
V647L
D
Control
WT A3
A3-R450Q
A3-I511V
A3-S527R
A3-S567R
A3-N587del
A3-L774S
O.D.
Time, min
β-lac Activity (% of WT)
WT A3
R450Q
I511V
S527R
S567R
N587del
L774S
E
Control
WT A4
A4-T639S
A4-A643G
A4-A644V
A4-R697P
O.D.
Time, min
β-lac Activity (% of WT)
WT A4
T639S
A643G
A644V
R697P

Figure-6

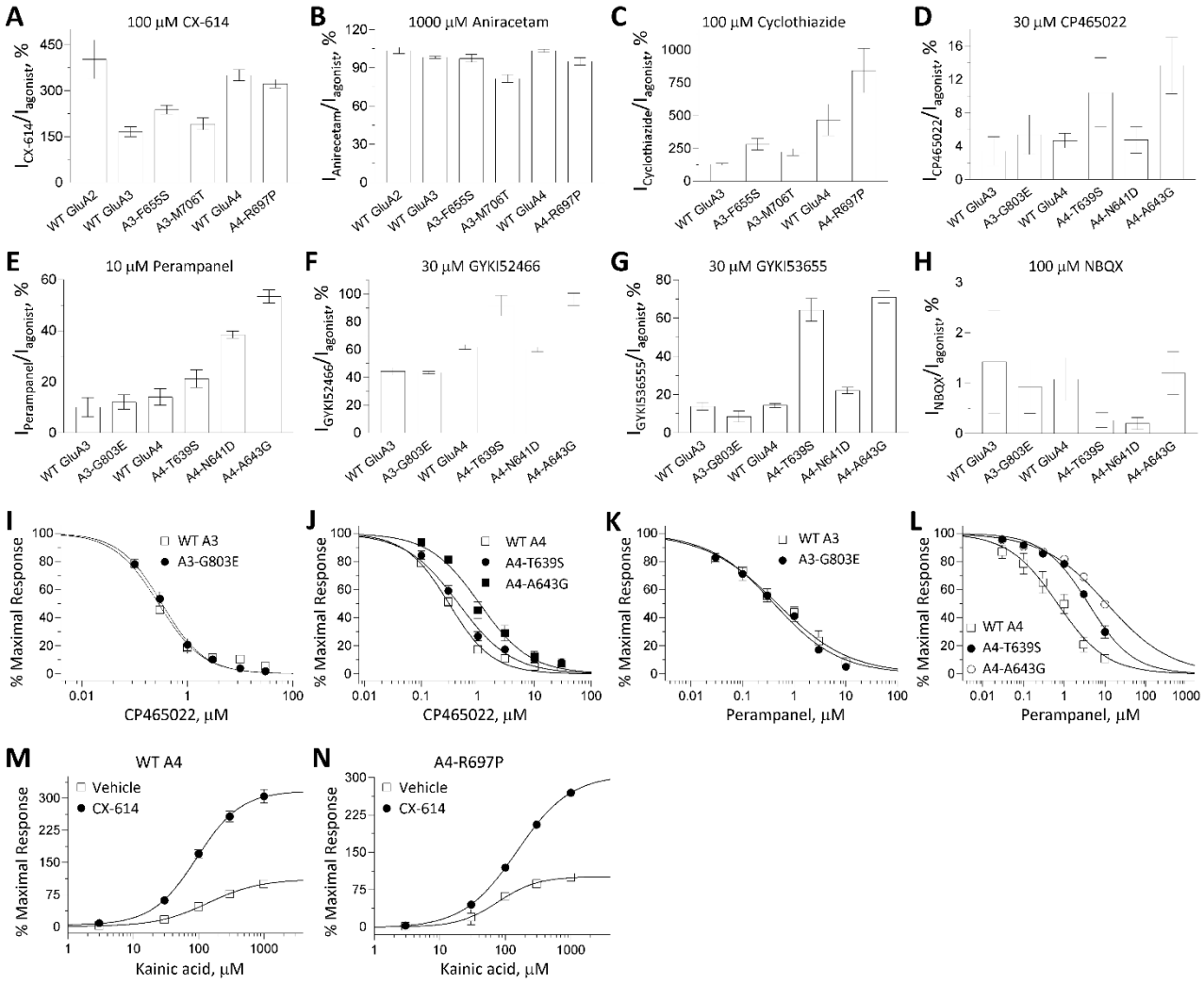
A
100 μM CX-614
I CX-614/I agonist, %
WT GluA2
WT GluA3
A3-F655S
A3-M706T
WT GluA4
A4-R697P
B
1000 μM Aniracetam
I Aniracetam/I agonist, %
C
100 μM Cyclothiazide
I Cyclothiazide/I agonist, %
D
30 μM CP465022
I CP465022/I agonist, %
WT GluA3
A3-G803E
WT GluA4
A4-T639S
A4-N641D
A4-A643G
E
10 μM Perampanel
I Perampanel/I agonist, %
F
30 μM GYKI52466
I GYKI52466/I agonist, %
G
30 μM GYKI53655
I GYKI53655/I agonist, %
H
100 μM NBQX
I NBQX/I agonist, %
I
WT A3
A3-G803E
% Maximal Response
CP465022, μM
J
WT A4
A4-T639S
A4-A643G
K
Perampanel, μM
L
M
WT A4
Vehicle
CX-614
Kainic acid, μM
N
A4-R697P